Journal of Chromatography A 1673 (2022) 463092

Contents lists available at ScienceDirect

Journal of Chromatography A

journal homepage: www.elsevier.com/locate/chroma

Review article

Reticular framework materials in miniaturized and emerging formats in analytical chemistry

Héctor Martínez-Pérez-Cejuela, Enrique Javier Carrasco-Correa, Ancuta Moga, María Vergara-Barberán, Miriam Beneito-Cambra, María Jesús Lerma-García, Ernesto Francisco Simó-Alfonso, José Manuel Herrero-Martínez*

CLECEM group, Department of Analytical Chemistry, University of Valencia, C/ Dr. Moliner, 50, 46100, Burjassot, Valencia, Spain

ARTICLE INFO

Article history:
Received 28 February 2022
Revised 29 March 2022
Accepted 1 April 2022
Available online 29 April 2022

Keywords:
Metal-organic frameworks
Covalent-organic frameworks
Off-site analysis
(Bio)sensing
Smart devices
Analytical applications

ABSTRACT

In recent years, important efforts have been put into miniaturization, coming on the scene formats such as chips, 3D-printed objects and paper-based devices. These systems have been applied to biological and chemical processes taking profit of their advantages such as waste reduction, low cost, portability, etc. Despite their benefits, there is a need to continue developing easier-to-use devices with enhanced performance addressed to face the current analytical challenges. In this sense, reticular porous materials such as metal- (MOFs) and covalent- (COFs) organic frameworks with unique features including tailorable porous architectures and tunable chemistry have attracted a lot of attention in various fields. Nevertheless, the combination of these materials with miniaturized and emerging formats has been scarcely investigated. This review is intended to bridge this gap and highlight the recent contributions of these materials in these analytical formats. Thus, this work aims to provide a comprehensive review of the field, highlighting incorporation strategies into the functional supports available to date, and the applications of the resulting systems in both off-site laboratory studies (mostly dedicated to (micro)extraction purposes) and on-site analysis. Finally, a discussion of challenges and future directions in this field is also given.

1. Introduction

Over the past decade, interest in the field of porous reticular materials, especially metal-organic frameworks (MOFs) and covalent-organic frameworks (COFs), has grown greatly due to their outstanding performance, which have led to broad applications including separation, catalysis, energy storage, sensing and biomedicine [1,2]. These reticular materials are characterized by crystalline structures (2D or 3D) with predefined topologies constructed by the combination of their precursors (Fig. 1A and 1B) linked by covalent or coordination bonds. MOFs are constructed from metal-based nodes (commonly inorganic salts) and organic ligands through strong coordination bonds, while COFs are exclusively made by organic molecules and non-metallic light elements (such as boron, carbon, silicon, nitrogen, and oxygen) [3]. Both materials have interesting properties such as attractive surface area (up to 10,000 m^2 g^{-1}), high porosity and large thermal and chemical stabilities, etc. In addition, the large number of available MOF/COF precursors allows the preparation of an endless number of these materials with devoted structures [4]. Moreover, MOFs and COFs can be post-synthetically modified to introduce additional tailorable functionalities (Fig. 1C), without changing the crystalline structure and encapsulation capacities. Their desirable characteristics make them excellent candidates for their application in analytical chemistry field for a wide variety of interests [1,5].

On the other hand, at present, material chemistry and analytical techniques tend to develop green, simple and low-cost approaches to reduce costs and minimize environmental impacts in agreement with Green Chemistry principles [6]. This issue can only be addressed if simple methodologies, complemented by comprehensive and reliable methods, are developed. This simplification must involve not only the instrumentation, but also the supporting materials used to obtain the results.

In this context, the miniaturization of devices has become in a promising strategy to achieve the portability in analysis systems. Microfluidic devices can be made using different materials such as glass, polymers and paper. In particular, the microfluidic paper-based analytical devices (μPADs) outstand for being affordable sub-

* Corresponding author.
E-mail address: jmherrer@uv.es (J.M. Herrero-Martínez).

https://doi.org/10.1016/j.chroma.2022.463092

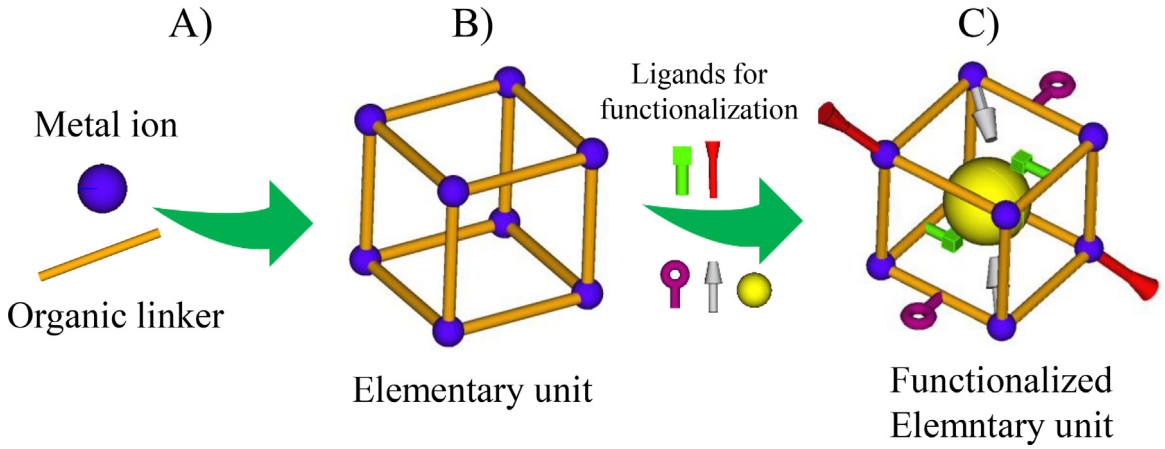

Fig. 1. Scheme of synthesis of MOFs and COFs and their post-functionalization.

strates with high availability [7]. Besides, PADs can be applied for microfluidic and quantitative colorimetric and electrochemical detection, producing reliable diagnostics in remote regions [8]. The rapid development of these miniaturized systems has been accompanied in recent years by the introduction of 3D printing into various fields of science to prepare solid structures with geometric precision for new equipment (scientific hardware) and manufacturing parts [9].

On the other hand, the combination of these miniaturized supports (such as chips) and emerging formats (like 3D printed devices and PADs) with the aforementioned materials have been scarcely explored. To the best of our knowledge, only few studies on the application of such a scenario have been described in the analytical chemistry field. From our point of view, this review could serve as a good starting point to learn about the rational use of these reticular materials in these new analytical formats. Regarding the structure of this review, it has been divided into several parts. The first section begins with a brief description of the design and preparation of MOFs and COFs. Next, an overview of different formats including chips, 3D printed devices and PADs is described. Then, the different strategies to incorporate MOFs and COFs into the functional supports will be commented. Subsequently, the applications of the abovementioned materials in these supports for off-site (mostly devoted to (micro)extraction purposes) and on-site analysis is described. Finally, a general conclusion as well as expected future trends of the hybridization of these materials with these formats is included.

2. Synthesis of MOF and COF materials

The development of a rational synthetic strategy is relevant to obtain MOFs and COFs with the desired properties for the selected analytical application. In this section, several general aspects related to the preparation of these reticular materials will be briefly introduced. For further details, the reader is referred to the existing body of literature [10–13].

Before proceeding with preparation aspects, it is worth mentioning that there is not a clear nomenclature for these materials. MOFs are termed with their precursors or named with the initials of the university where they were discovered, such as MIL (Materials Institute of Lavoisier), HKUST (Hong Kong University of Science and Technology) or ZIF (Zeolitic Imidazole Framework). On the other hand, COFs are usually named using their precursor abbreviations.

Regarding the synthesis of MOFs [11,12], several synthetic approaches can be followed such as slow diffusion [14,15], solvothermal (including hydrothermal) [16,17], electrochemical [18,19], mechanochemical [20,21] or using greener processes [22] such as microwave- and ultrasound-assisted methods [23]. Among them, the most popular is the solvothermal method. Usually, a Teflon-lined bomb is used as the reaction vessel, and the raw materials (metal ions and commercially available or pre-synthesized linkers) are added into the vessel. The reaction occurs in a small scale and takes an appropriate duration depending on the specific conditions. The as-synthesized MOFs are generally washed with a solvent, activated and/or dried before its characterization and use.

Via careful selection of their constituents, MOFs can meet the necessary attributes to address specific demands. In this sense, the wide number of combinations between metal centers and organic linkers, and the availability of various synthesis and modification strategies, open up a large array of possibilities for the preparation of MOFs suitable for the capture, separation or determination of a target analyte. To date, the number of experimentally known structures of MOFs has been already almost 80, 000 [24]. In analytical chemistry field, the use of MOFs has been extensively applied with sample treatment purposes, although other interesting features of these materials such as fluorescence [25], catalytic behavior [26], conducting solids [27], biomimetic mineralization [28], and supercapacitors [29] have been reported.

On the other hand, COFs are commonly built by the combination of symmetric and rigid organic molecules. Indeed, the topological type and pore structure of the COFs are mainly determined by the shape, length and symmetry of their precursors [10,13]. Thus, many organic compounds have been successfully designed for constructing COFs, such as boric acids, phenols, amines, aldehydes, ethers, acid anhydrides and ketones. Fig. 2 shows some examples of organic precursors used for synthesis of certain COFs.

Regarding the approaches for the construction of COFs, some of the synthetic routes includes solvothermal [30], microwave [31], room-temperature synthesis (vapor assisted) [32], among others have been described [33,34]. Just like MOFs, the solvothermal synthesis is the most usual method to fabricate COFs. Overall, these materials have interesting features of lower density and higher stability in acid-basic media compared with MOFs due to the organic nature of their precursors and the only presence of covalent bonds. On the other hand, taking into account the particular building unit geometries, the preparation of 2D structures is more common than the 3D structures (predominant in MOFs), resulting in lower surface areas [34]. Furthermore, there are only certain conditions and precursors that can be used to create COF structures, which reduces the number of these structures compared to the reported MOFs.

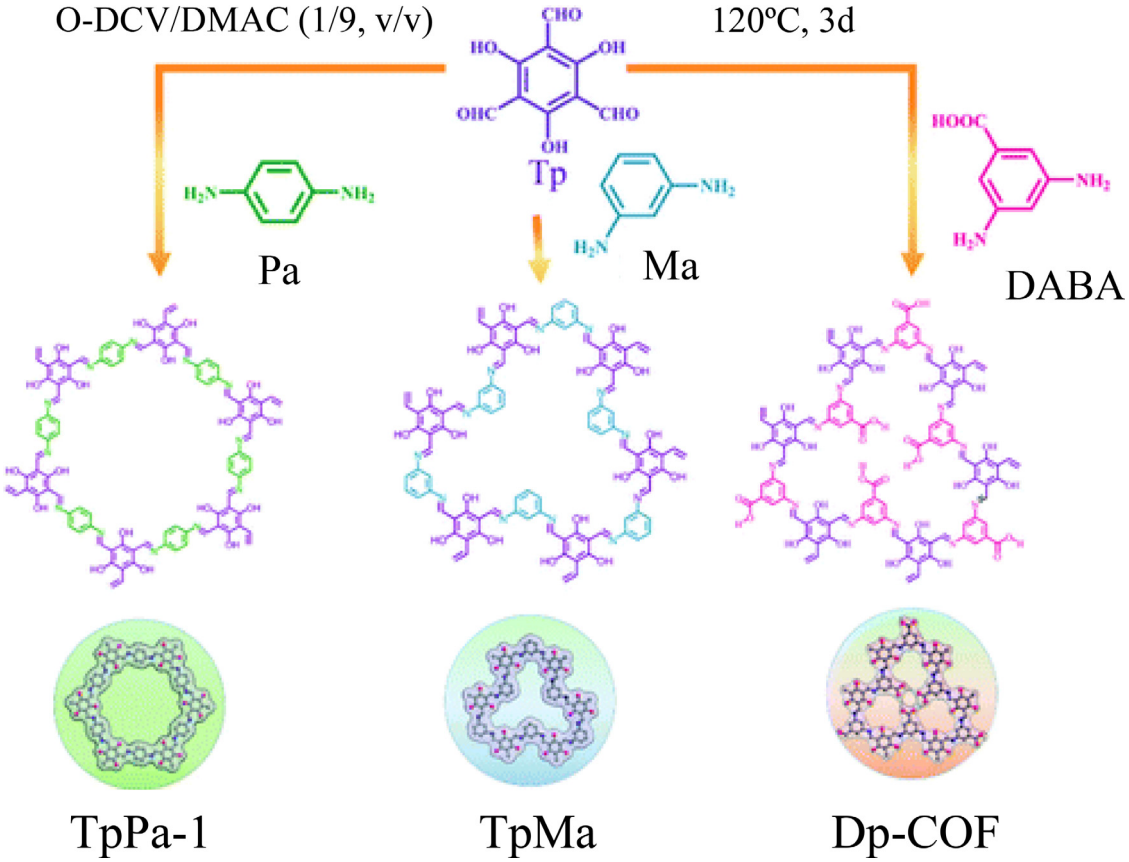

Fig. 2. Examples of some precursors used for the syntheses of COFs and the influence of their topology (including their 2D skeleton). Abbreviations: *o*-DCB: 1,2-Dichlorobenzene; DMAC: N, N-dimethylacetamide; Tp: 2,4,6-trihydroxy-1,3,5-benzenetriformaldehyde; Pa: p-Phenylenediamine; Ma: m-phenylenediamine; DABA: 3,5-diaminobenzoic acid. Reprinted from Zhang et al. [112] with permission of the Royal Society of Chemistry.

3. Miniaturized and emerging low-cost formats for analytical chemistry

As we mentioned in the Introduction, the miniaturization of analytical methodologies continues being a topic of major concern. Reducing dimensions of conventional analytical systems is not the only driving force toward miniaturization, but also achieving benefits such as lower reagent and sample consumption, automation, portability, among others. In this context, several miniaturized platforms have been addressed both to sample treatment purposes [35] and to integrate several steps of the analytical process, such as micro total analysis system (μTAS) [36].

In the last two decades, most of microfluidic devices have been built in poly(dimethylsiloxane) (PDMS) by soft lithography, a technique based on PDMS micromolding, which allows an easy building of complex fluidic channels at microscale [37]. Fig. 3A shows the most common approach used for the fabrication of PDMS-based devices. Once the mold is prepared, the PDMS pre-polymer solution is poured to the mold and then solidified by heating. After removing the PDMS layer from the mold, the PDMS could be bond with a glass layer with the aid of oxygen plasma to seal the microchannels. This polymer has gained an important edge as material for microfluidic device preparation due to its key features such as reduced cost, biocompatibility, optical transparency, elastomeric properties, and high precision to prototype complex designs [37]. However, the fabrication process of PDMS microchips typically involves large human effort, which tends to make these systems difficult to expand outside of research laboratories, and the layered molding constrains the complexity of the devices that can be produced [38]. Besides, the control systems required to run these microfluidic devices usually imply engineering expertise and equipment do not present in most routine laboratories.

Currently, there is an increasing focus on the development of technologies able to manufacture reliable and efficient devices that can be rapidly prototyped with low-cost per unit, and with negligible energy consumption and minimal expertise requirements. In this context, 3D-printing has recently attracted attention as such smart way to fabricate miniaturized systems and the possibility to print design intricate patterns due to its automated, assembly-free 3D fabrication, very reduced costs, availability, variety of printing technologies and materials [39,40].

Regarding printing technologies, fused deposition model (FDM), vat polymerization (stereolitography (SLA) and digital light processing (DLP)), photopolymer inkjet printing (PIP), and selective laser sintering (SLS) have been used. Fig. 3B shows a scheme of some of these 3D printing technologies. Briefly, in FDM, a heated thermoplastic material is extruded and deposited layer-by-layer until device construction. In vat polymerizations, a UV curable epoxy or acrylic-based resin is polymerized on a mobile platform spot-by-spot (SLA) or layer-by-layer (DLP). PIP technology uses a combination of vat polymerizations and FDM technologies, allowing the use of multiple materials with high accuracy. Meanwhile, SLS is based on sintering a deposited metal or other materials onto a solid support achieving high-precision objects. From these techniques, FDM and SLA have been the most widely used to manufacture analytical components and smart multifunctional devices. For more extensive information about the benefits and limitations of these 3D printing techniques, the reader is referred to several recent reviews [41,42]. Despite the merits of 3D printing,

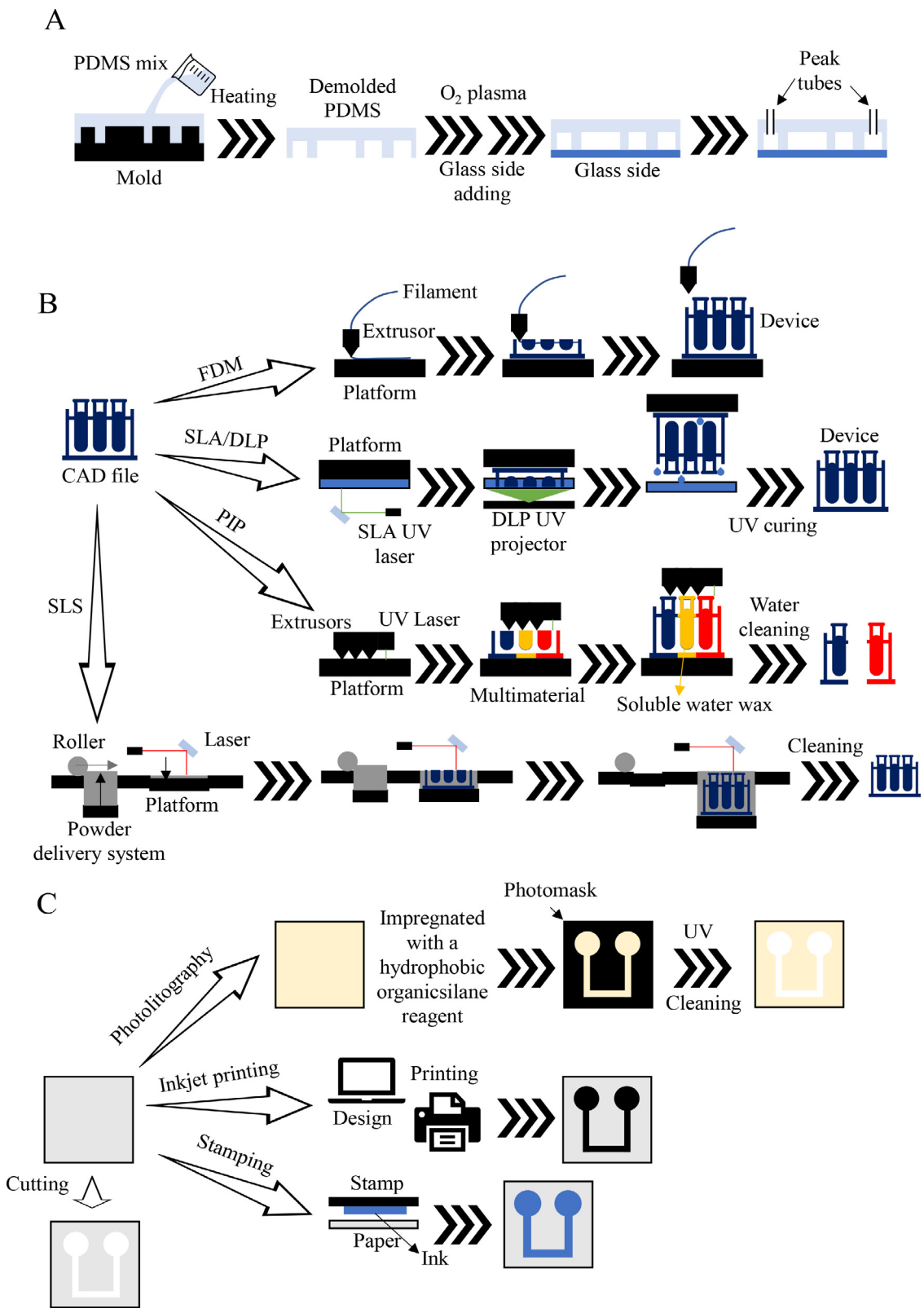

Fig. 3. Schematic examples of the most common approaches for preparation of PDMS-based microchips (A), 3D printed objects (B) and µPADs (C).

this technology also shows several handicaps such as low resolution of microstructures (particularly, microfluidic channels), limited choice of printable materials (with good solvent compatibility and transparency) and need for post-printing processes (curing and/or cleaning) [42]. In any case, the impact of 3D printing in the field of microfluidic devices as well as in the sample preparation area is still at an early stage [43].

Other type of promising and cost-effective technology is that based on PADs (or paper-based platforms). Due to its intrinsic properties such as versatility, inherent capillary flow, portability,

miniaturization, biocompatibility, among others [44], the use of cellulose paper as substrate has attracted great attention.

Within PADs, microfluidic PADs (μPADs) have undergone innovative developments over the last decade due to their advantageous feature such as simple fabrication (without cleanroom facilities), ability to process small volumes of fluids and perform multiplexed assays, and do not require external pumps to operate compared to the traditional microfluidic devices. μPADs are fabricated by patterning paper with hydrophobic barriers to define hydrophilic channels and reaction zones.

There are many techniques for patterning paper [45], such as photolithography, wax/inkjet printing, stamping, and cutting, etc. Fig. 3C shows a schematic representation of some of these approaches. Briefly, photolithography consists in the transferring of a geometric structure in a photomask to a light-sensitive photoresist impregnated in the paper. Wax printing is accomplished by printing wax patterns on the paper surface and heating the wax through the paper. In the case of inkjet printing, a UV curable ink is used to pattern the microfluidic channels into the paper, which are generated after a curing process. On the other hand, the stamping mode is based on forming hydrophobic ink channels by handmade, using a PDMS stamp with an indelible ink. Other technique used is by cutting paper through high-cost X-Y plotters or CO_2 lasers, which offer sharp defined features. In any case, these patterning techniques have been well-introduced in several reviews [44,46], thus they will not be covered here in detail. These μPADs or other paper-based platforms have been used together with spectroscopic, electrochemical and mass spectrometric (MS) detection [47], and in some of these approaches have been addressed to the development of point-of-care (POC) diagnostic assays. Apart from the use of PADs for the development of bio(sensing) applications, other important role of paper has been its use as a substrate for the preparation of sorptive phases in micro SPE. A comprehensive overview of these microextraction applications has been recently published [47].

4. Incorporation of reticular materials in miniaturized and emerging formats

Different strategies have been reported for the incorporation of MOFs and COFs in the different types of abovementioned supports.

Regarding chips, different supports such as poly(ethylene terephthalate) [48], PDMS [49–52], glass [53,54], titanium gold nanotubes (TiAuNTs) [55], acrylate [56,57], and even gold- [58] and nickel-based [59] chips have been used to incorporate MOFs. A common way to introduce these materials has been performed by directly embedding MOFs in microchannels [50,53] using slurries of MOF (nano)particles and introduced them into the channels by controlling microvalves or (micro)pumping systems. However, this approach is rather limited due to variations in packing quality, dependence of chip substrate, high backpressures, clogging, etc. Besides, careful and tedious conditions are needed to provide proper packed beds without microchip damage. An interesting way, developed by some authors [52,55-57], has been the use of a dispersion of magnetic MOF flushed through the microcolumn using a syringe pump in combination with the application of an external magnet to trap the material in the microfluidic system. Other alternative developed in certain kind of chips, such as surface-enhanced Raman scattering (SERS) substrates, has been the deposition of MOF on substrates previously modified with metal nanoparticles (NPs) [48,54,58,59].

In general, for chip-MOF hybridization, MIL [52,53,55,57] and ZIF [48,54,56] MOF families have been commonly used, although other materials such as MOF-74 [60], UiO-66 [50,61] and HKUST-1 [49] have been also employed.

On the other hand, the common approach to incorporate MOFs in the 3D-printed parts is by blending the pre-synthesized MOF particles into 3D printing polymer in order to create 3D printed MOF/COF-based composites [62–66]. This approach has been usually employed in FDM printers [64,67-69], although other techniques such as DLP [62], SLA [70] and SLS [63] have been also adopted. However, this later approach gave composites with MOF crystals partially embedded in the thermoplastic scaffold, which is detrimental to the performance of the device. Alternatively, MOFs have been *in situ* grown by post-printing modification using layer-by-layer approach on already preformed 3D printed supports [71]. Nevertheless, this strategy is limited to 3D printable materials able to absorb metals to initiate MOF growth and is such time-consuming procedure. In this context, recent approaches have been addressed to overcome these limitations through the *in situ* growth of MOF from metal precursors [67,68,72]

Recent efforts to introduce reticular materials on 3D printed devices relied on: i) the introduction of the as-synthesized MOF in the 3D printing pre-mixture [63,64], ii) 3D printable filament containing MOF metal oxide precursor followed by MOF conversion [68], iii) the use of magnetic MOF composites [70], iv) 3D printable hydrogel precursor inks (with incorporated MOF organic linkers) [72], or v) the use of sealing agents to introduce the reticular materials in the final composite [60,73].

Concerning PADs as support, cellulose-based papers have been selected as the preferred option [74–98] because of their high and easy availability (such as Whatman #1), among other interesting features. Furthermore, carbon [61,99], cellulose acetate filters [100], well-plate device [101] or paper strips [102,103] have been selected to prepare paper-based supports for specific applications. The common strategies to incorporate reticular materials to paper substrate are based on the physical deposition of a dispersion containing the synthesized MOF crystals [75,77,81-84,90,93,98,102,104] or through the immersion of the paper into this dispersion [85,87-90,96,101,102]. In this sense, the use of adhesive agents such as chitosan [74,79], polyvinyl alcohol (PVA) [86,91,94], agar [103] or starch [97] in the solution have been proposed to immobilize MOFs or COFs on paper. For instance, a PVA coating of paper was done to later attach some MOFs such as Ni-MOF [86], Zr-PCN-222(Fe) [94] or Eu-MOF [91] crystals onto the surface. These strategies are simple and fast, although they require highly stable MOF dispersions to produce a homogeneous distribution of the material in the final substrate. Alternatively, other less explored strategies such as the *in situ* growth of the desired MOF onto paper surface [80] and attachment via conjugation bonds [92,95,100] could be good choices to hybridize MOF and paper substrates thus maximizing the interaction with analytes and controlling the width of MOF layer. For example, Hou et al. [78] developed a sensor with dual-mode detection of volatile sulfur compounds in exhaled breath. In so doing, a carboxymethylation of the cellulose paper was carried out with chloroacetate and sodium hydroxide in order to coordinate Cu(II) ions easily after a washing step with deionized water. In any case, these latter approaches could involve more preparation time than those based on simple deposition/immersion, although the resulting phases can lead to very stable coatings.

4.1. Miniaturized and emerging formats containing MOFs/COFs for off-site applications

In this section, the use of abovementioned formats containing MOFs or COFs as selective materials aimed at off-site (bio)analytical applications will be described (Table 1). Within chip-based supports, few reports have been described in combination with MOFs for remote applications [50-52,54,57-59]; and, there are only two reports on applications with COFs [105,106].

Table 1
Summary of developed emerging tools for off-site applications (LOD: limit of detection; RSD: relative standard deviation; R.: recovery/removal; L.R.: linear range; P.F.: preconcentration factor; S.V.: sample volume; A.T.: adsorption time; Sto.: storage; Re.: reusability; A.C.: adsorption capacity).

MOF/COF information			Format	Analytes / Sample	LOD / RSD (%)	Remarkable features[1]	Ref.
Name	**Anchorage**	**Function**					
Chips combined with MOFs							
Fe_3O_4@SiO_2@UiO-66-SH	Embedding	Adsorption	PDMS chip for ICP-MS	Arsenic species / SCC-7 Cell	6.6-13.5 ng L^{-1}/ <6.1	L.R.: 0.02-20 µg L^{-1}; P.F.: 23-25; Selective	[50]
AuNPs@AgNPs@ZIF-8	Deposition	Adsorption	ITO-glass chip with SERS detection	Carbendazim / seawater	0.2 µg kg^{-1}/ <9	R.: 88-102 %; L.R.: 1 nM-10 µM Good stability; Sto.: 35 d	[54]
Fe_3O_4@MIL-101(Fe)@ anti-hCG	Magnetic	Adsorption	Acrylate- based chips with SERS detection	hCG protein / human urine	0.61 IU L^{-1} / <15	R.: 101-110 %; S.V.: 15 µL; A.T.: 1 h; Selective; Reusable	[57]
Cu-TCPP 2D MOF	Au coordination	Signal enhancement	Gold chip with electrochemical detection	PD-L1 exosomes / human serum	16.7 particles mL^{-1} / <15	R.: 93-102 %; 39.57°/RIU increase; Selective	[58]
S-MOF@Au	Au coordination	Signal enhancement	Ni sheet chip with Raman detection	Food contaminants / food products	15-1000 nM / <10	R.: 96-125 %; L.R.: 10-10^6	[59]
Au@CuO/Cu-MOF	Sealing	Catalyst	PDMS chip with electrochemical detection	NO / cancer cells	7.8 nM /<6	L.R.: 0.03–500 μM; Selective; Sto.: 1 month;	[51]
Immune PtNPs@NH_2-Fe-MIL-88(Fe)	(Bio)recognition and magnetic	Catalyst	PDMS chip with electrochemical detection	*Salmonella* / chicken	93 CFU mL^{-1} / -	R.: 91-116%; L.R.: 1.01•10^2 - 1.01•10^6 CFU mL^{-1}; A.T.: 1 h; Selective	[52]
Chips combined with COFs							
Tfpa–Mth COF	*In-situ* growth	Adsorption	Quartz crystal microbalance chip	Fe(III) / ethanol	64 nM / -	Selective	[105]
Bpda-Bth COF	*In-situ* growth	Adsorption	Quartz crystal microbalance chip	Hg(II) / water	58 nM / -	L.R.: 5–50 μM; Selective; Re.: 5 cycles	[106]
3D Printed objects combined with MOFs							
HKUST-1	Embedding	Adsorption	DLP 3D printed extraction device	MB / -	-/ -	Enhanced mechanical and water stability; A.C.: ~ 0.7 mg g^{-1}	[62]
ZIF-8, NH_2-MIL-101(Al) HKUST-1, ZIF-67, MOF-801	Embedding	Adsorption	SLS 3D printed extraction device	MB / -	- / -	Removal enhancement: 5-fold; MOF content: 10-40 wt. %; Re.: 5 cycles	[63]
HKUST-1	Embedding	Adsorption	Sodium alginate based resin with colorimetric detection	Dyes / water	- / -	R.: 96-100 %; A.T.: 20 min; MOF content: 12.96 wt %; Printing geometry studies; Re.: 7 cycles	[64]
Ca-MOF/graphite powder/paraffin	Deposition	Adsorption	3D-printed syringe-type integrated device	Pb(II) / fish feed and tap water	0.26 g L^{-1} / <6	R.: 97-102%; L.R.: 0-130 µg L^{-1}; Selective; Sto.: 3 months;	[65]
graphite paste/Ca-MOF	Deposition	Adsorption	Lab-in-a-syringe device	Hg(II) / fish oil and tap water	0.6 μg L^{-1} / <5	R.: 98-101%; A.C.: 255 mg g^{-1}; pH applicability: 3-8; Selective; Sto.: 2 months	[66]
Ca-MOF	*In-situ* growth	Adsorption	$CaSiO_3$/ABS/TPU Inkjet 3D printing device	Methylene blue / water	- / -	R.: 80-88 %; A.T.: 300 min; MOF content: 3.2 wt.%; Re.: 6 cycles	[67]
ZIF-8	*In-situ* growth	Adsorption	ZnO-NP/ABS 3D printed device with colorimetric detection	Malachite green / water	- / <5	R.: 90-99%; A.T.: 5h; MOF content: 10 wt.%; Re.: 6 cycles	[68]
Fe_3O_4@MOF-5	Magnetic	Adsorption	SLA 3D printed microfluidic device for LC-MS/MS	Fluoroquinolones / milks	9-12 ng L^{-1}/ <7	R.: 95-105%; L.R.: 0.5-1000 ng mL^{-1}	[70]
HKUST-1	*Layer-by-layer* growth	Adsorption	PLA 3D printing piece with colorimetric detection	Malachite green / waste water	- / -	R.: 90-93%; Synthesis: 8 layers; A.T.: 10 min; Re.: 3 cycles	[71]
HKUST-1	*In-situ* growth	Adsorption	Inkjet 3D printing device	Methylene blue and rhodamine B / water	-/ -	R.: 33-96%; High mechanical stability; Selective	[72]
UiO-66-SO_3H@Ag	Sealing	Adsorption	Methacrylate 3D-printed piece with gamma spectrometry detection	^{131}I / sewage and hospital waste water	- / <10	R.: 90-98%; A.C.: ~1 MBq g^{-1}, Re.: 3 cycles	[73]
3D Printed objects combined with COFs							
COF-GO foams	Embedding	Adsorption	3D-printed piece	Dyes, $KMnO_4$, bisphenol A / water	- / -	R.: <80 %; A.T.: 60 s; pH work range: 1-11; Selective; Re.: 5 cycles	[108]
Fe_3O_4@COF@BSA/3DE	Covalent	Signal enhancement	3D-printed nanocarbon electrode	L-Tryptophan / racemic mixture	- / -	Chiral recognition of enantiomers via H-bonds	[69]

(*continued on next page*)

Table 1 (*continued*)

MOF/COF information			Format	Analytes / Sample	LOD / RSD (%)	Remarkable features[1]	Ref.
Name	**Anchorage**	**Function**					
Chit-CP@MIL-101(Cr)	Sealing	Adsorption	Qualitative filter paper for LC-MS/MS	Triazine herbicides / environmental water	1.5-22 ng L^{-1} / <13	R.: 77-125%; L.R.: 0.5-50 ng mL^{-1}; A.T.: 15 min	[74]
GNR-QD@NU-901	Deposition	Adsorption	Cellulose paper-based thin-film microextraction with fluorescence and SERS detection	Benzaldehyde / exhaled breath	0.05 mg L^{-1} / <15	L.R.: 0.002-5 mg L^{-1}; Stability: after 160 min of laser excitation and under high humidity; Sto.: 10 weeks	[75]
Ni-MOF@AuNPs@ CNTs@PVA	Sealing	Adsorption	Cellulose membrane film electrode	HIV DNA / human serum	0.13 nM / <7	R.: 96-104%; L.R.: 10 –1000 nM; High mechanical stability: Selective; Re.: 200 cycles; Sto.: 20d	[86]
Pd@Hollow Zn/Co Core–Shell ZIF67/ZIF8	(Bio)conjugation	Signal enhancement	Filter paper (whatman #2) with colorimetric and electrochemical detection	Prostate-Specific Antigen / human serum	0.78 ng L^{-1} / <3	L.R.: 5-50000 ng L^{-1}; Selective; Sto.: 28 d;	[92]
MIP/Fe_3O_4/C-dots@Ag-MOFs.	Deposition	Signal enhancement	Cellulose chromatographic coupled to chip with electrochemical detection	Parathion-methyl / vegetables, fruits, soil and water	11.6 pM / <5	R: 83-109 %; L.R.: 50-20000 pM; Selective; Sto.: 1 month	[93]
GOx@Zr-PCN-222(Fe)@PVA	Sealing	Encapsulation and catalyst	Filter paper (whatman #1) with colorimetric detection	Glucose / water	0.25 mM /-	L.R.: 0-5 mM; A.T.: 2-3.5 h; 10% of encapsulation; 10-15% turnover efficiency	[94]
S1-AuNP@Cu-BDC	Conjugation	Encapsulation and catalyst	Filter paper (whatman #1) with electrochemical detection	miRNA-155 / human serum	0.35fM / <6	R.: 94-100%; L.R.: 1 fM-10 nM; Selective; Sto.: 30 d	[95]
Co/Mo-MOF	Deposition	Formation of Mo-chromophore	Ashless filter paper strips with colorimetric detection	As(V) / ground water	0.02-0.04 µg L^{-1} /-	R.: 97-104%; A.T.: 15 min	[96]
PADs combined with COFs							
Starch@TpBD	Sealing	Adsorption	Filter paper in SPME for PS-MS	TBBPA / water	1 nM (LOQ) /<3	R.: 95-102%; P.F.: 50; A. T.: 8.5 min Sto.: 35 d	[97]

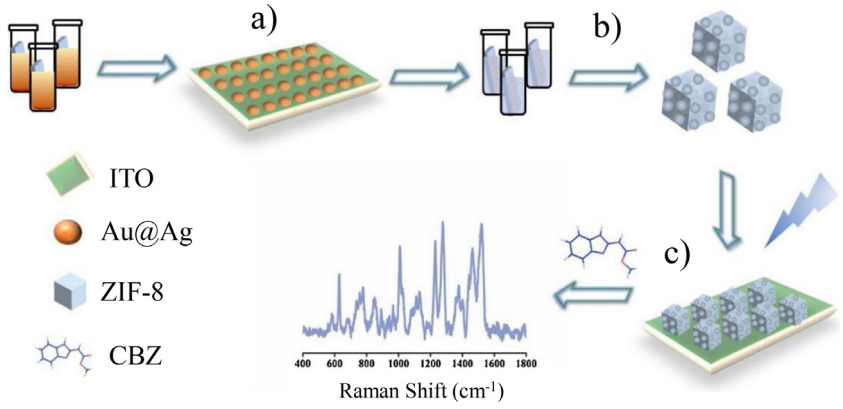

Fig. 4. Scheme of preparation ITO-Au@Ag@ZIF-8 chip and analysis of carbendazim using this device. a) Silver-coated AuNP assembly on ITO glass; b) immersion of ITO-Au@Ag sheet into MOF precursor solution and subsequently ZIF-8 growth; c) SERS detection of CBZ. Reproduced from Zhai et al. [54] with permission from Elsevier.

For instance, Zhai et al. [54] have prepared a ZIF-8 MOF onto SERS chips to determine carbendazim (CBZ) in seawater. For this purpose, the authors prepared a chip (Fig. 4) using a pre-treated indium tin oxide (ITO) coated glass (with amino-silanized groups in its surface), which was used as substrate for attachment of Au@Ag nanoparticles. Then, $ZnNO_3$ and 2-methylimidazole (HMIM) were used as building units for the *in-situ* preparation of ZIF-8 MOF onto the ITO-modified chip (ITO-Au@Ag chip). The ITO-Au@Ag@ZIF-8 chip showed a limit of detection (LOD) of 0.2 µg kg^{-1}, two order of magnitude lower than the ITO-Au@Ag chip. Moreover, the LOD achieved was better than that obtained by other conventional methods (HPLC-fluorescence detection, 0.55 µg kg^{-1}; SERS, 12.5 µg kg^{-1}; electrochemical, 57.4 µg kg^{-1}). However, the developed device was not able to reach the LODs obtained using aptasensors [107]. The resulting signal enhancement can be explained taking into account the interaction between CBZ and ZIF-8, and surface plasmon resonance effect of neighbouring Au@Ag NPs within the valley of ZIF-8 MOF nanoparticles. Unfortunately, no data about chip-to-chip reproducibility was provided, and any comment about chip regeneration/reuse was included in this work.

Another interesting example is provided by Ahi et al. [57], who developed magnetic MOF NPs modified with human chorionic gonadotropin antibody (Ab-hCG) to isolate and pre-concentrate this protein using a permanent magnet. The magnetic MOF captured hCG was then transferred in a capillary driven microfluidic chip, which was used as SERS-based platform. Recoveries of hCG in urine samples close to 100% and LOD as low as 0.61 IU L^{-1} were found. A remarkable strength of the proposed protocol is its

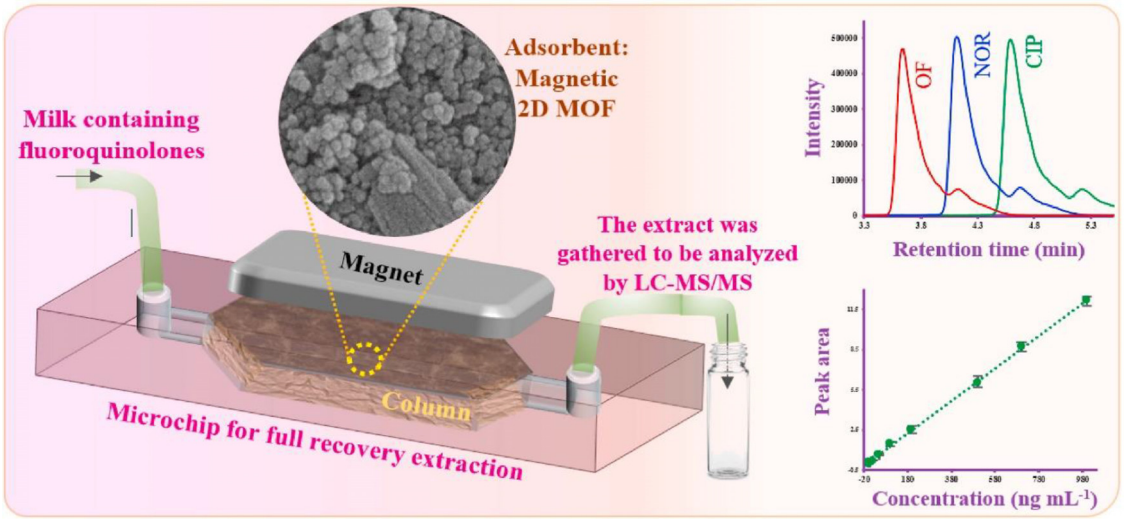

Fig. 5. Magnetic MOF magnetically retained in the 3D printed chip for FQs extraction in milk samples followed by LC-MS/MS analysis. Reproduced from Bagheri et al. [70]with permission from Elsevier.

shorter sample processing and analysis time (1 h) in comparison to the traditional methods (e.g. LC-MS, ELISA, Western Blotting) for hCG detection, which is utmost interest for doping control.

Also, it is worth to mention two contributions from the same group [105,106], in which COF-based microchip methodologies using quartz crystal microbalances (QCM) as platforms for the detection of inorganic ions (Fe(III) and Hg(II)). After surface functionalization of QCM substrate, the COF was anchored via *in-situ* growth, thus allowing a direct interaction between COF and analytes. Both studies showed an excellent selectivity and low LODs (~ 10-100 nM) for monitoring of metal ions.

With regards to 3D-printed supports, different designs have been adopted to prepare efficient devices in combination with MOFs for a wide range of applications (Table 1). In most of these reports, HKUST-1, prepared from cupper salts and benzene-1,3,5-tricarboxylic acid (BTC) as precursors, has been one of the most widely prepared MOFs in the 3D-printed devices due to its synthesis in mild conditions avoiding the chemical compatibility issues of 3D-printed parts [62-64,72]. To date, most of the published articles devoted to the fabrication of MOF-polymer materials have been focused on the removal of harmful dyes (such as cationic dye methylene blue) from aqueous solutions [62-64,67,68,72]. However, its extension to sample pre-treatment or other analytical purposes has been scarcely explored, and it would be highly desirable. In this sense, removal of other harmful contaminants including heavy metals [65,66], antibiotics [70], radioisotopes [73] have been also stated. Finally, it is also remarkable that the use of COFs in combination with 3D printing technology has been addressed to enantioseparation of L-tryptophan [69] and the removal of dyes, $KMnO_4$ and bisphenol A with the same COF-based device [108]. Taking a closer look at an example of the potential of hybridization between 3D printing and MOFs for sample preparation is illustrated in the extraction of fluoroquinolones (FQs) in milk prior to HPLC-MS/MS determination described by Bagheri et al. [70]. The authors designed and printed a polymer-based fluidic support containing a microcolumn filled with MOF. In particular, a magnetic MOFs was synthesized by the reaction of Zn(II) and terephthalic acid in the presence of magnetic NPs. Then, the dispersed solution of sorbent was delivered into the microcolumn, and it was fixed in the fluidic device using two magnets (Fig. 5). This configuration works like a common SPE cartridge, but it avoids the use of retaining frits. Under optimized conditions, the developed method showed high recoveries (95-105%) in milk samples, satisfactory precision values (RSD < 4.3%), and low LODs (9-16 ng L^{-1}), although no device-to-device reproducibility was evaluated. Despite of benefits (easy operation, less toxic solvent usage, etc.) of this configuration for extraction purposes, certain details such as information of resin nature and .STL file (design) were missing.

Concerning the preparation of paper-based sorptive phases containing reticular materials, few works [74,75,86,92-97] have been described (Table 1). In any case, from this table, cellulosic paper is clearly the most widespread substrate used for the fabrication of sorptive phases in thin-film microextraction (TFME). The hybridization of reticular materials with the paper platform is commonly addressed by direct deposition of the pristine MOF/COF or combined with sealing agents. However, this approach can lead to losses of the material, thus affecting the reusability of devices. Alternatively, a modification of paper substrate with hazard oxidant reagents to provide chelating sites for in situ synthesis of MOF/COF crystals. Concerning to detection modes, spectroscopic (colorimetric) and electrochemical schemes have been preferentially used taking into account their low cost and versatility.

An interesting application was described by Jiang et al. [74], who has developed a cellulose paper coated with a MOF of type MIL-101(Cr) as extraction phase in TFME for triazine herbicides prior to their quantification by HPLC-MS/MS. For this purpose, the cellulose paper was successfully coated with the MOF MIL-101(Cr) in a chitosan (Chit) matrix prepared by one-step vacuum filtration. Subsequently, the coated paper was cut into circular pieces (diameter 1.5 cm) placed in a polypropylene tube with sample solution and vortexed. After parameters optimization of TFME parameters (including mass ratio of MIL-101(Cr)/Chit ratio, sample pH, adsorption/desorption time, type and volume of desorption solvent), the method was applied to environmental water samples achieving recovery values ranged from 77 to 125%. an acceptable reproducibility (RSD values < 13%), and low LODs (1.5-22.0 ng L^{-1}). This study showed that MIL-101(Cr)/Chit-modified paper can also be applied to extract other related compounds (containing heteroatoms or aromatic rings in their structure) thanks to MOF surface chemistry. Nonetheless, one of the main drawbacks of the proposed sorbent was its film fragility, which seriously limits its use in other extraction techniques (e.g., ultrasonic assisted extraction).

An interesting application using COFs for PADs preparation has been developed by Zhang and his group [97]. In this work, a COFs-based paper coupled with paper spray mass spectrometry (PS-MS) to determine tetrabromobisphenol A (TBBPA) in water samples

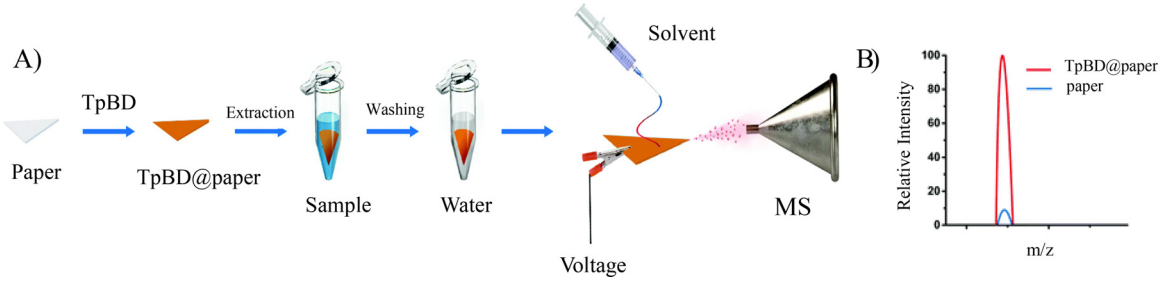

Fig. 6. A) Schematic representation of the preparation of TpBD-coated paper, the SPE protocol and posterior coupling with PS-MS. B) Signal enhancement after application of COF-coated paper. Reproduced from Zhang et al. [97] with permission from The Royal Society of Chemistry.

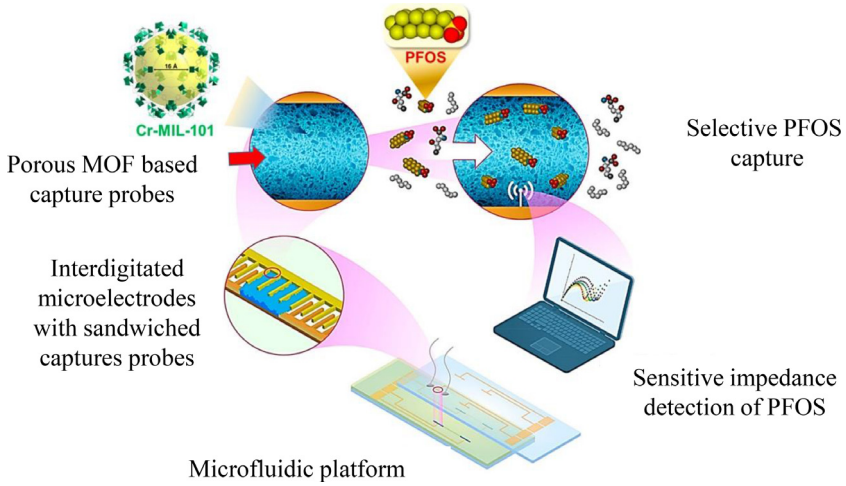

Fig. 7. Scheme of PFOS detection using a LOC device using a MOF-based capture probe. Reproduced from Chen et al. [53] with permission from American Chemical Society.

is described (Fig. 6). The COF was firstly synthesized from 1,3,5-triformylphloroglucinol (Tp) and benzidine (BD) and then added to a starch solution (crosslinking agent). The resulting solution gave a TpBD coating on the paper using the vacuum filtration method. The presence of COF enhanced the analytical performance comparing with bare paper. The COFs-coated paper coupled with PS-MS exhibited a large selectivity, satisfactory recoveries (95-102%), low LOD (0.3 nmol L^{-1}, a 50-fold enhancement compared with the naked paper substrate), and good reproducibility (paper-to-paper RSD < 3.0%) for the detection of TBBPA. Also, the TpBD-coated paper showed a long-time stability (at least 35 days) without losing its performance.

4.2. Incorporation of MOFs/COFs in emerging tools for on-site applications

The aforementioned formats can be combined with MOF/COF materials to prepare on-site systems to be applied in the (bio)analytical field. Table 2 shows the most recent examples of applications on-site devices containing MOFs, since no reports have been detailed with COF materials.

Lab-on-a-chip (LOC) can be considered as one of the most common on-site devices [109]; however, its combination with these reticular materials has been scarcely studied [49,53,55,56,61]. This fact can be explained by the need of external accessories (such as thermostat and micropumps), thus restricting applicability in on-site uses. Within these few applications, it is remarkable that developed by Chen and coworkers [53]. The authors introduced Cr-MIL-101 MOF inside a microfluidic channel, sandwiched between interdigitated microelectrodes (Fig. 7). This MOF was used as the probe for the targeted perfluorooctanesulfonate (PFOS) capture based on the affinity of the chromium center toward both the fluorine tail groups as well as the sulfonate functionalities. Thanks to the hybridization, a significant increase of sensitivity was achieved (LOD of 0.5 ng L^{-1}). This value was superior to previous in situ analytical PFOS sensors and comparable to LODs achieved by sophisticated techniques (LC-MS/MS) [110]. The practical applicability of this device was successfully tested for in situ determination of PFOS in groundwater matrices.

Also, few articles have been published combining 3D printing with MOFs for on-site applications [60,65,66,111]. In these manuscripts, 3D printing technology has been mainly aimed at constructing micro/milifluidic supports [60,65,66] and smartphone adaptors [111]. An interesting example of smartphone-interfaced 3D printed sensor integrating MOF for portable and sensitive measuring Fe(III) has been described by Zhao et al. [111]. Thus, hydroxyl functionalized fluorescent MOFs (MIL-53(Fe)-$(OH)_2$) were prepared and used as probes. The pore of the MOFs and the specific binding interaction between Fe(III) and hydroxyl led to a fast response of the fluorescent intensity quenching (Fig. 8A). Then, a smartphone-based fluorescent reader was fabricated by assembling different 3D printed components to construct a POC platform (Fig. 8B). The results obtained from this portable platform exhibited great detection sensitivity (LOD of 1.7 µM) compared with a commercial microplate reader. Besides, the as-prepared sensor was successfully applied to determine Fe(III) in human serum and environmental water samples with satisfactory recovery values (90-109%).

As we mentioned in the Introduction, PADs with their multiple advantages have revolutionized on-site sensing field in the last decade; and some articles using MOFs aimed at this topic have been described (Table 2). Thus, MOFs have been recognized as excellent platforms for implementation in PADs used with different purposes as preserving the biorecognition capability of immobi-

Table 2
Summary of the on-site emerging devices containing MOFs (LOD: limit of detection; RSD: relative standard deviation; R.: recovery/removal; L.R.: linear range; P.F.: preconcentration factor; S.V.: sample volume; A.T.: adsorption time; Sto.: storage; Re.: reusability).

MOF/COF information			Format	Analytes / Sample	LOD / RSD (%)	Remarkable features[1]	Ref.
Composite name	**Anchorage**	**Function**					
Chips combined with MOFs							
AgNPs@HKUST-1	Deposition	Adsorption	PDMS chip with surface-enhanced Raman scattering detection	PAHs / environmental waters	0.15-20 nM / <9	R.: 80-118%; L.R.: 0.5 nM-5 M; Cyclable; Selective	[49]
MIL-101(Cr)	Embedding	Adsorption	Glass microfluidic chip and electrochemical detection	PFOS / groundwater	0.15 ng L^{-1} / -	R.: 95%; S.V.: 5 mL; A.T.: 144 h	[53]
Fe_3O_4@ZIF-4	Magnetic	Adsorption	Acrylate-based microchips with chemiluminescence detection	Phenolic acids and flavonoids / tea and honey	40-100 µg L^{-1} / <5	R.: 95-104%; L.R.: 0.1-10 µg L^{-1}; Selective	[56]
rGO@SWCNTs/ NH_2-UiO-66@PEI	Deposition	Adsorption	Screen printed carbon electrode and electrochemical sensor	Cd(II), Cu(II), Hg(II), Pb(II) / water	0.025-0.351 µM/<8	R.: 88-147%; L.R.: 0.5-10 µM; Selective; Cost 10 $; Weight 30 g	[61]
PdNPs@ZIF-67	Deposition	Catalyst	PET chip with electrochemical detection	Glucose / perspiration	2 µM / <3	Maintenance-free perspiration monitoring; Flexible sweatband device; Real-time analysis; Long-term stability (up to 2 months)	[48]
GOx-Apt@m-MIL-100(Fe)	Magnetic	Generation of intracellular iron ions	TiAuNTs semiconductor electrode chip	Tumor cells / -	2 cell mL^{-1} / -	R.: 90-99%; L.R.: 2-5000 cell mL–1; All-in-one system;	[55]
3D Printed objects combined with MOFs							
$(OH)_2$-MIL-53(Fe)	*In-situ* growth -	Adsorption	3D printed smartphone adaptor with fluorescence detection	Fe(III) / River water, human blood and living cells	1.7 µM / -	R.: 90-109 %; L.R.: 5-200 µM; Selective	[111]
Mn-MOF	Sealing	Signal enhancement	3D printed microfluidic with electrochemical detection	Cd(II) and Pb(II) / plastic products	0.2-0.5 µg L^{-1} / <5	R.: 95-102%; L.R.: 0.5-100 µg L^{-1}; Selective; Flexible Connected to iPad via a USB to enable real-time;	[60]
Ca-MOF	Embedding	Working electrode/cation exchange	3D printing support with electrochemical detection	Pb(II) / fish feed and tap water	0.26 µg L^{-1} / <6	R.: 97-102%; L.R.: 0-130 µg L^{-1}; A.T.: 360 s; Selective; Sto.: 3 months	[65]
Ca-MOF	Embedding	Working electrode/cation exchange	3D printing support with electrochemical detection	Hg(II) / fish oil and tap water	0.6 µg L^{-1} / <5	R.: 98-101 %; L.R.: 2-40 µg L^{-1}; A.T.: 360 s; Lab-in-a-syringe device; Selective; Sto.: 2 months	[66]
PADs combined with MOFs							
MoS_2@HKUST-1	Deposition	Adsorption	Cellulose paper with electrochemical detection	H_2O / exhaled breath	- / -	Sleep apnea diagnosis with sensor embedded mask. Monitoring via app; A.T.: ~0.38 s; Sto.: 1 month	[98]
Ab@ZIF-8	Deposition	Adsorption	Filter paper (Whatman #1) with colorimetric detection	IgG and IgM / human serum	1 ng mL^{-1} (PBS) 200 ng mL^{-1} (serum) /-	Reusable DI water pH 6; Sto.: 30 d;	[76]
Apt@UiO-66	Deposition	Adsorption and signal enhancement	Paper-based disposable screenprinted electrode	Cancer-derived exosomes / exosome-free fetal bovine serum	$5•10^3$ particles mL^{-1} /	R.: 95-102%; L.R.: $1.7•10^4$ -$3.4•10^8$; A. T.: 80 min; Selective; Sto.: 5 weeks	[77]
Cu-TATB MOF	Coordinated	Adsorption and catalyst	Filter paper (Whatman #1) with colorimetric and chemiluminescence detection	volatile sulphur compounds / exhaled breath	8 nM and 0.2 µM / <2	R.: 90-110%; L.R.: 10–400 μM; Selective; Sto.: 18 months (in air); A.T.: ~30 min	[78]
DNA@Pt NPs@Cu-MOF	(Bio) conjugation	Signal enhancement	Cellulose acetate membrane filter with electrochemical detection	mi-RNA-141 and -21 / human serum	0.1 fM / <5	R.: 93-108%; Selective; Storage: 30 d	[100]
Chit@MIL-101(Fe)	Sealing	Catalyst	Plastic-backed cellulose paper with colorimetric detection	Glucose / human serum and urine	2.5 μmol•L^{-1} / <2	R.: 93-109%; L.R.: 10-150 µM; Selective; Sto.: 21 d	[79]
Co-MOF/CC/Paper	*In-situ* growth	Catalyst	Filter paper (Whatman #1) with electrochemical detection	Glucose / human serum, urine and saliva	0.15 mM / <12	R.: 87-109%; L.R.: 0.8–16 mM; Selective; Sto.: 60 d	[80]
Luminol@ZIF-67	Deposition	Catalyst	Filter paper (Whatman #1) with chemiluminescence detection	Catechol / tea and tap water	1.1 mg L^{-1} / <4	R.: 95-108 %; L.R.: 5-100 mg L^{-1}; Selective; S.V.: 5 µL; Sto.: 30 d	[81]
GOx-Co-MOF	Deposition	Catalyst and increase stability	Filter paper (Whatman) with fluorescence and colorimetric detection	Glucose / human blood	3.2-16.3 µM / <4	R.: 95-105%; L.R.: 50-15000 µM; Signal stability: 2 h; Selective; Sto.: 20 d	[82]

(*continued on next page*)

Table 2 (*continued*)

MOF/COF information			Format	Analytes / Sample	LOD / RSD (%)	Remarkable features[1]	Ref.
Composite name	**Anchorage**	**Function**					
[Eu0.05/Tb0.95]-MOF	Deposition	Fluorescence activity	Filter paper (Whatman #1) with fluorescence detection	pH and water content / -	0.1% (v/v) / -	L.R.: 0-0.8% (H_2O, v/v); Stable; Re.: 5 cycles	[83]
[Eu0.125/Tb0.875]-MOF	Deposition	Fluorescence activity	Filter paper (Whatman #1) with fluorescence detection	2,6-dipicolinic acid / human serum	19.1 µM / <2	R.: 99-102%; L.R.: 40-100 mM; Selective; Sto.: 2 d	[84]
RhB@Al-MOF	Deposition	Fluorescence activity	Filter paper (Whatman #1) with fluorescence detection	Malachita green / Crucian and grass carp	1.6 mg L^{-1} / <7	R.: 91-109 %; L.R.: 0.5–200 mg L^{-1}; Selective; A.T.: ~5 min; Sto.: 15 d	[85]
CdTe-QDs@NH_2-MIL-88(Fe)	Deposition	Fluorescence activivty	Filter paper (Whatman) with fluorescence detection	Hg(II) and Cu(II) / red wine	0.22-0.26 ng mL^{-1} / <5	R.: 92-109%; L.R.: 10-5000 ng mL^{-1}; Selective	[87]
Eu-BDC and Eu-DPA MOFs	Deposition	Fluorescence activivty	Fiber Whatman paper microchips with fluorescence detection	H_2O_2 / water and milk	0.14 µM / <10	R.: 88-106 %; L.R.: 0.001-1 mM; S.V.: 5 µL; A.T.: 20 min; Selective; Sto.: 30 d	[88]
$(OCOCH_3)_2$-NH_2-UiO-66	Deposition	Fluorescence activivty	Filter paper (Whatman #1) with fluorescence detection	Hydrazine / environmental waters	10^{-8} M / -	Selective; P.F.:14-fold A.T.: 1 min	[89]
PVA@Eu-MOF	Sealing	Fluorescence activivty	Filter paper with fluorescence and logic detection	Eu(III) and fluoride / groundwater	0.25-1.15 µM / -	R.: 95-103%; L.R.: 0-515 µM; Selective	[91]
1-OHP@Co/Tb-DPA MOF	Deposition	Fluorescence activity	Well plate with Whatman sensing paper with fluorescence detection	pH / gastric juices	- / <7.3%	L.R. (pH): 0.3-7.8; A.T.: 30 s; S.V.: 5 µL; Selective; Sto.: 30 d Re.: 6 cycles	[101]
Tb(III)@Al-MOF	Deposition	Fluorescence activity	Test strips with fluorescence detection	p-aminophenol / human urine	5 µg mL^{-1} /<6	R.: 88-94%; L.R.: 0.005-5 mg mL^{-1}; Selective; Re.: 5 cycles	[102]
Agar@Eu-TATB MOF	Sealing	Fluorescence activity	Paper strip with colorimetric detection	Sulfamethazine / water	0.67 µM / <6	R.: 100-110 %; L.R.: 0 to 50 μM; A.T.: ~mins; Selective; Re.: 5 cycles	[103]
Zn-MOF	Deposition	Fluorescence activity	Common filter paper with fluorescence detection	Aristolochic acids / human serum and urine	0.004 μM / -	R.: 99-100%; Water stable MOF (> 5 days) Selective; Re.: 4 cycles	[104]
Tb(III)@Cd-MOF	Deposition	Encapsulation and energy transfer	Filter paper with fluorescence detection	Arginine / human urine	0.69 mg L^{-1} /-	L.R.: 1 µM-10 mM; Selective; A.T.: 20 s; Re.: 5 cycles	[90]

lized biomolecules [76,77,90,100], acting as a catalyst [79–82], and mostly in sensing of different species such as organic compounds using MOF with fluorescence activity [84,85,87-89,91,102-104] and pH [83,101]. Among these studies, it is important to remark the work described by Ortiz-Gómez and collaborators [79]. The authors reported for the first time the use of MOF as a peroxidase mimetic in μPAD. Using the peroxidase mimic advantage of MIL-101(Fe), the authors prepared a glucose colorimetric sensor by MOF deposition onto a commercial cellulose paper. The peroxidase-like catalytic activity of this MOF can be attributed to unsaturated coordination sites created by water removal from trimeric clusters, and the large pores of this framework, which favors an easy access to Fe(III), which acts as Lewis acid catalyst. The PAD developed by the authors consisted of three separate zones: one for sampling; the second one is a transport channel, where a mixture of glucose oxidase and buffer were deposited; lastly, a detection zone, where the chromogenic reagent and MOF were placed. The images of resulting colored product were taken with smartphone and analyzed yielding a correlation with glucose concentration. The µPAD showed low LODs (2.5 μmol•L^{-1}), acceptable linear range (10-150 μmol•L^{-1}), satisfactory recoveries (93-109%) in serum and urine samples, and good selectivity in presence of common biological compounds. Besides, in this study, it has been demonstrated that the implementation of MOFs in paper-based systems presents advantages in terms of cost (0.03 cents per unit), durability (at least 21 days), and stability (MOF robustness) compared with other existing glucose determination methods.

Concerning to sensing systems in PADs, luminescent MOFs (especially lanthanide MOFs) have been the common choice to prepare portable systems with enhanced sensitive recognition. As an example, Qin et al. [102] has developed an interesting work using a fluorescence doped Tb(III)-MOF, which was deposited in paper strips. A smartphone was used for selectively p-aminophenol (PAP) detection as phenylamine biomarker in urine samples (Fig. 9). It should be highlighted that the detection can be easily followed by naked eye thanks to a quantitative colour change. This sensor allowed the home monitoring of PAP (around 90% of recoveries) in a wide range (0.005-5 mg mL^{-1}) with low LOD (5 μg mL^{-1}). Also, acceptable reusability (5 times), good selectivity (Fig. 9) and stability were achieved. Its convenience as a POC device was supported by short response time (< 5 min) and simple recycling step with deionized water.

4. Current challenges and future perspectives

Despite the potential of these reticular materials, several challenges still remain in improving their effective incorporation in miniaturized analytical devices. Reasonable control and adjustment of the morphology/structure and functionality of MOFs/COFs is always a great issue to improve the final performance of sorptive or (bio)sensor devices. In so doing, the introduction of simple and green synthesis protocols should be considered in order to produce sustainable analytical devices. In this sense, the room temperature synthesis, microwave irradiation or other available techniques (together with non-toxic reagents) to create mild conditions should open new avenues to obtain sustainable materials.

Concerning the analytical platforms, the fabrication of low-cost microfluidic devices should be encouraged, playing 3D-printing technology a relevant role in the development of modular mi-

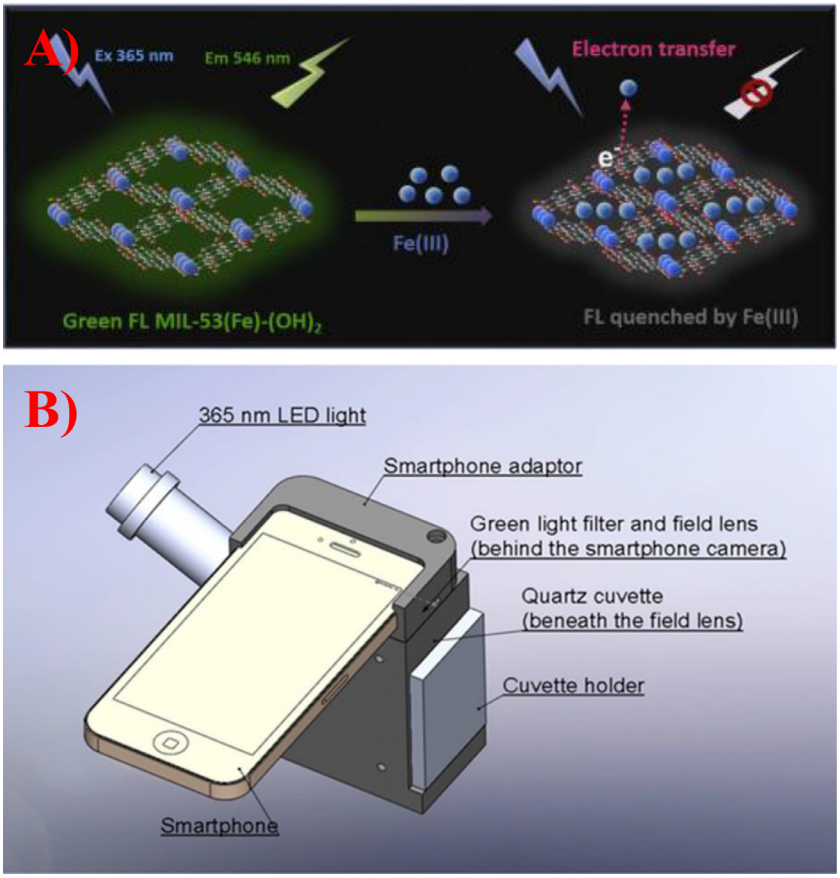

Fig. 8. (A) Scheme illustration of the quenching mechanism of MIL-53(Fe)-$(OH)_2$ in the presence Fe (III), and (B) 3D printed smartphone adaptor for on-site fluorescent reader. Reproduced from Zhao et al. [111] with permission from Elsevier.

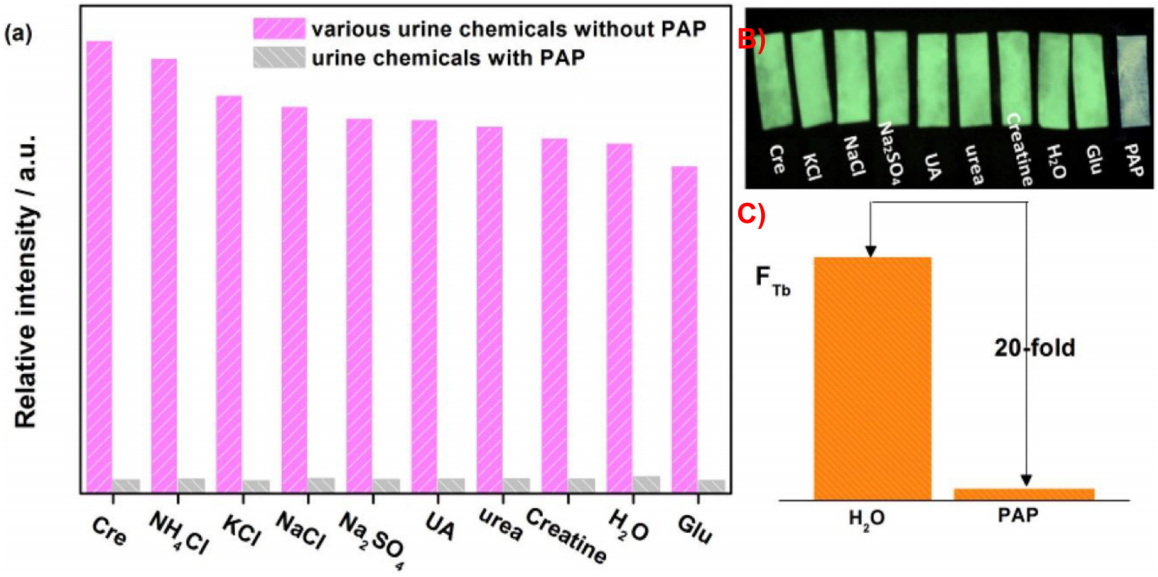

Fig. 9. A) Selectivity study of relative fluorescence intensity of Tb(III)-MOF in presence of PAP (quenching effect) and different possible interferences in urine matrix. B) Tb(III)-MOF coated strip response to PAP presence with coexistent matter under 365 nm UV radiation. C) Comparison of Tb(III)-MOF fluorescence signal with deionized water and PAP standard solution. Reproduced from Qin et al. [102] with permission from Elsevier.

crofluidic systems. For future developments, resolution needs to be further enhanced in the field of 3D printing along with development of more user-friendly support materials. Also, certain inherent qualities of μPADs should be improved to improve its robustness and reproducibility through the development of enhanced preparation methods.

Other key aspect that deserves more research is the incorporation approaches of these materials in the different formats. Some current strategies compromise the crystalline structure and blocked/reduced the number of active sites of these materials. For instance, 3D printing technique has been used to shape MOF/COF powder as manipulable; however, the versability of 3D printing

should be improved developing novel approaches (*e.g.* through the use of precursor of MOF/COFs, as was discussed in Section 3) able to incorporate higher reticular material loading.

Also, the MOF/COF-based supports need to meet the reusability demand in order to achieve a sustainable development and expand their applicability. Indeed, information on current uses of these devices is missing or rarely reported. Consequently, research and development efforts to address this issue include the application of diverse techniques/process for reuse and regeneration of these reticular materials such as activation of MOFs by heat, vacuum, solvent exchange, supercritical carbon dioxide and other miscellaneous options.

Lastly, other additional issue to be considered is the stability and shelf-life of the final devices, particularly those that use biological assays for analysis. Research focused on studying the shelf life of these materials has produced some promising results, but additional research is needed in this area. In this sense, we believe that the number of MOF/COF-based materials with more optimized and stable structures will be increased in the coming years to produce flexible and functional devices with enhanced properties for sample preparation and (bio)sensing applications.

5. Concluding remarks

In this review, the current status of the use of MOF/COFs in microfluidic chips, 3D-printed objects and μPADs has been considered, providing comprehensive and important insights into the manufacturing materials, incorporation strategies and applications of the resulting devices in off-site developments and on-site analysis. Concerning off-site purposes, the use of MOFs in these formats has been mainly addressed to sample preparation with most works devoted to the preparation of adsorbents. On the other hand, MOFs have shown great potential for on-site analysis due to their useful properties (e.g. signal-transduction capability, luminescence, etc.). Conversely, few works have been published on both topics using COF-based materials, being still in their infancy. In any case, we believe that in the near future, specific functional COFs will be further developed for these analytical applications.

Declaration of Competing Interest

The authors declare that they have no known competing financial interests or personal relationships that could have appeared to influence the work reported in this paper.

CRediT authorship contribution statement

Héctor Martínez-Pérez-Cejuela: Conceptualization, Investigation, Writing – original draft, Writing – review & editing. **Enrique Javier Carrasco-Correa:** Conceptualization, Investigation, Writing – original draft. **Ancuta Moga:** Writing – review & editing. **María Vergara-Barberán:** Writing – review & editing. **Miriam Beneito-Cambra:** Writing – review & editing. **María Jesús Lerma-García:** Writing – review & editing. **Ernesto Francisco Simó-Alfonso:** Supervision, Writing – review & editing, Resources, Funding acquisition. **José Manuel Herrero-Martínez:** Conceptualization, Supervision, Writing – review & editing, Resources, Funding acquisition.

Acknowledgments

This study was supported by the project (RTI2018-095536-B-I00) funded by MCIN/AEI/10.13039/501100011033 and by "ERDF A way of making Europe" by the European Union. H. Martínez-Pérez-Cejuela thanks the Ministry of Science, Innovation and Universities of Spain (MSIU) for a PhD FPU contract (ref. FPU18/02179). María Vergara-Barberán also thanks the Generalitat Valenciana for a VALi + D postdoctoral research contract (ref. APOSTD/2020/213). This article is based upon work from the Sample Preparation Study Group and Network, supported by the Division of Analytical Chemistry of the European Chemical Society.

References

[1] I. Pacheco-Fernández, P. González-Hernández, J. Pasán, J.H. Ayala, V. Pino, The rise of metal-organic frameworks in analytical chemistry, Handb. Smart Mater. Anal. Chem. (2019) 463–502, doi:10.1002/9781119422587.ch15.
[2] B. Rajender, M.I. Ahamed, M.A. Abdullah, Application of metal-organic frameworks and their derived materials, Jonh Wiley & Sons, 2020.
[3] O.M. Yaghi, Reticular chemistry in all dimensions, ACS Cent. Sci. 5 (2019) 1295–1300, doi:10.1021/acscentsci.9b00750.
[4] M.J. Kalmutzki, N. Hanikel, O.M. Yaghi, Secondary building units as the turning point in the development of the reticular chemistry of MOFs, Sci. Adv. 4 (2018) eaat9180, doi:10.1126/sciadv.aat9180.
[5] X. Wang, N. Ye, Recent advances in metal-organic frameworks and covalent organic frameworks for sample preparation and chromatographic analysis, Electrophoresis 38 (2017) 3059–3078, doi:10.1002/elps.201700248.
[6] M. de la Guardia, S. Garrigues, Handbook of green analytical chemistry, John Wiley & Sons, 2012.
[7] Y. Yang, E. Noviana, M.P. Nguyen, B.J. Geiss, D.S. Dandy, C.S. Henry, Paper-Based Microfluidic Devices: Emerging Themes and Applications, Anal. Chem. 89 (2017) 71–91, doi:10.1021/acs.analchem.6b04581.
[8] C. Parolo, A. Merkoçi, Paper-based nanobiosensors for diagnostics, Chem. Soc. Rev. 42 (2013) 450–457, doi:10.1039/c2cs35255a.
[9] A.K. Au, W. Huynh, L.F. Horowitz, A. Folch, 3D-Printed Microfluidics, Angew. Chemie - Int. Ed. 55 (2016) 3862–3881, doi:10.1002/anie.201504382.
[10] P.J. Waller, F. Gándara, O.M. Yaghi, Chemistry of Covalent Organic Frameworks, Acc. Chem. Res. 48 (2015) 3053–3063, doi:10.1021/acs.accounts.5b00369.
[11] H. Furukawa, K.E. Cordova, M. O'Keeffe, O.M. Yaghi, The chemistry and applications of metal-organic frameworks, Science 341 (80) (2013) 1230444, doi:10.1126/science.1230444.
[12] M. Safaei, M.M. Foroughi, N. Ebrahimpoor, S. Jahani, A. Omidi, M. Khatami, A review on metal-organic frameworks: Synthesis and applications, TrAC - Trends Anal. Chem. 118 (2019) 401–425, doi:10.1016/j.trac.2019.06.007.
[13] C.S. Diercks, O.M. Yaghi, The atom, the molecule, and the covalent organic framework, Science 80 (2017) 355, doi:10.1126/science.aal1585.
[14] J.Y. Wu, T.C. Chao, M.S. Zhong, Influence of counteranions on the structural modulation of silver-di(3-pyridylmethyl)amine coordination polymers, Cryst. Growth Des. 13 (2013) 2953–2964, doi:10.1021/cg400363e.
[15] L. Piñeiro-López, Z. Arcís-Castillo, M.C. Muñoz, J.A. Real, Clathration of five-membered aromatic rings in the bimetallic spin crossover metal-organic framework [Fe(TPT)2/3{MI(CN)2}2]•G (MI = Ag, Au), Cryst. Growth Des. 14 (2014) 6311–6319, doi:10.1021/cg5010616.
[16] Y. Zhang, X. Bo, A. Nsabimana, C. Han, M. Li, L. Guo, Electrocatalytically active cobalt-based metal-organic framework with incorporated macroporous carbon composite for electrochemical applications, J. Mater. Chem. A. 3 (2015) 732–738, doi:10.1039/c4ta04411h.
[17] L. Shen, W. Wu, R. Liang, R. Lin, L. Wu, Highly dispersed palladium nanoparticles anchored on UiO-66(NH2) metal-organic framework as a reusable and dual functional visible-light-driven photocatalyst, Nanoscale 5 (2013) 9374–9382, doi:10.1039/c3nr03153e.
[18] T.R.C. Van Assche, G. Desmet, R. Ameloot, D.E. De Vos, H. Terryn, J.F.M. Denayer, Electrochemical synthesis of thin HKUST-1 layers on copper mesh, Microporous Mesoporous Mater 158 (2012) 209–213, doi:10.1016/j.micromeso.2012.03.029.
[19] N. Campagnol, E. Rezende Souza, D.E. De Vos, K. Binnemans, J. Fransaer, Luminescent terbium-containing metal-organic framework films: new approaches for the electrochemical synthesis and application as detectors for explosives, Chem. Commun. 50 (2014) 12680–12683, doi:10.1039/c4cc05742b.
[20] D.A. Haynes, T. le Roex, Mechanochemical synthesis of an yttrium based metal-organic framework, Chem. Commun. 49 (2013) 972, doi:10.1039/c2cc36325a.
[21] D. Lv, Y. Chen, Y. Li, R. Shi, H. Wu, X. Sun, J. Xiao, H. Xi, Q. Xia, Z. Li, Efficient Mechanochemical Synthesis of MOF-5 for Linear Alkanes Adsorption, J. Chem. Eng. Data. 62 (2017) 2030–2036, doi:10.1021/acs.jced.7b00049.
[22] H. Reinsch, Green" Synthesis of Metal-Organic Frameworks, Eur. J. Inorg. Chem. (2016) 4290–4299, doi:10.1002/ejic.201600286.
[23] N.A. Khan, S.H. Jhung, Synthesis of metal-organic frameworks (MOFs) with microwave or ultrasound: Rapid reaction, phase-selectivity, and size reduction, Coord. Chem. Rev. 285 (2015) 11–23, doi:10.1016/j.ccr.2014.10.008.
[24] Cambridge Crystallographic Data Center (CCDC). https://www.ccdc.cam.ac.uk/structures/, 2021-01-26. (n.d.), 2020.
[25] Y. Liu, X.Y. Xie, C. Cheng, Z.S. Shao, H.S. Wang, Strategies to fabricate metal-organic framework (MOF)-based luminescent sensing platforms, J. Mater. Chem. C. 7 (2019) 10743–10763, doi:10.1039/c9tc03208h.
[26] V. Pascanu, G. González Miera, A.K. Inge, B. Martín-Matute, Metal-organic frameworks as catalysts for organic synthesis: A critical perspective, J. Am. Chem. Soc. 141 (2019) 7223–7234, doi:10.1021/jacs.9b00733.

[27] S.K. Bhardwaj, N. Bhardwaj, R. Kaur, J. Mehta, A.L. Sharma, K.H. Kim, A. Deep, An overview of different strategies to introduce conductivity in metal-organic frameworks and miscellaneous applications thereof, J. Mater. Chem. A. 6 (2018) 14992–15009, doi:10.1039/c8ta04220a.
[28] K. Liang, R. Ricco, C.M. Doherty, M.J. Styles, S. Bell, N. Kirby, S. Mudie, D. Haylock, A.J. Hill, C.J. Doonan, P. Falcaro, Biomimetic mineralization of metal-organic frameworks as protective coatings for biomacromolecules, Nat. Commun. 6 (2015) 7240, doi:10.1038/ncomms8240.
[29] B. Xu, H. Zhang, H. Mei, D. Sun, Recent progress in metal-organic framework-based supercapacitor electrode materials, Coord. Chem. Rev. 420 (2020) 213438, doi:10.1016/j.ccr.2020.213438.
[30] M. Matsumoto, R.R. Dasari, W. Ji, C.H. Feriante, T.C. Parker, S.R. Marder, W.R. Dichtel, Rapid, Low Temperature Formation of Imine-Linked Covalent Organic Frameworks Catalyzed by Metal Triflates, J. Am. Chem. Soc. 139 (2017) 4999–5002, doi:10.1021/jacs.7b01240.
[31] H. Wei, S. Chai, N. Hu, Z. Yang, L. Wei, L. Wang, The microwave-assisted solvothermal synthesis of a crystalline two-dimensional covalent organic framework with high CO2 capacity, Chem. Commun. 51 (2015) 12178–12181, doi:10.1039/c5cc04680g.
[32] D.D. Medina, J.M. Rotter, Y. Hu, M. Dogru, V. Werner, F. Auras, J.T. Markiewicz, P. Knochel, T. Bein, Room temperature synthesis of covalent-organic framework films through vapor-assisted conversion, J. Am. Chem. Soc. 137 (2015) 1016–1019, doi:10.1021/ja510895m.
[33] M.S. Lohse, T. Bein, Covalent Organic Frameworks: Structures, Synthesis, and Applications, Adv. Funct. Mater. 28 (2018), doi:10.1002/adfm.201705553.
[34] K. Geng, T. He, R. Liu, S. Dalapati, K.T. Tan, Z. Li, S. Tao, Y. Gong, Q. Jiang, D. Jiang, Covalent organic frameworks: design, synthesis and functions, Chem. Rev. 120 (2020) 8814–8933, doi:10.1021/acs.chemrev.9b00550.
[35] F.A. Hansen, S. Pedersen-Bjergaard, Emerging Extraction Strategies in Analytical Chemistry, Anal. Chem. 92 (2020) 2–15, doi:10.1021/acs.analchem.9b04677.
[36] J.B. Nielsen, R.L. Hanson, H.M. Almughamsi, C. Pang, T.R. Fish, A.T. Woolley, Microfluidics: innovations in materials and their fabrication and functionalization, Anal. Chem. 92 (2020) 150–168, doi:10.1021/acs.analchem.9b04986.
[37] K. Raj M, S. Chakraborty, PDMS microfluidics: A mini review, J. Appl. Polym. Sci. 137 (2020) 1–14, doi:10.1002/app.48958.
[38] K. Raj M, S. Chakraborty, PDMS microfluidics: A mini review, J. Appl. Polym. Sci. 137 (2020), doi:10.1002/app.48958.
[39] P.N. Nesterenko, 3D printing in analytical chemistry: Current state and future, Pure Appl. Chem. 92 (2020) 1341–1355, doi:10.1515/pac-2020-0206.
[40] C.L. Manzanares Palenzuela, M. Pumera, (Bio)Analytical chemistry enabled by 3D printing: Sensors and biosensors, TrAC - Trends Anal. Chem. 103 (2018) 110–118, doi:10.1016/j.trac.2018.03.016.
[41] B. Gross, S.Y. Lockwood, D.M. Spence, Recent advances in analytical chemistry by 3D printing, Anal. Chem. 89 (2017) 57–70, doi:10.1021/acs.analchem.6b04344.
[42] E.J. Carrasco-Correa, E.F. Simó-Alfonso, J.M. Herrero-Martínez, M. Miró, The emerging role of 3D printing in the fabrication of detection systems, TrAC - Trends Anal. Chem. (2021) 136, doi:10.1016/j.trac.2020.116177.
[43] L. Wang, M. Pumera, Recent advances of 3D printing in analytical chemistry: Focus on microfluidic, separation, and extraction devices, TrAC - Trends Anal. Chem. 135 (2021) 116151, doi:10.1016/j.trac.2020.116151.
[44] T. Ozer, C. McMahon, C.S. Henry, Advances in Paper-Based Analytical Devices, Annu. Rev. Anal. Chem. 13 (2020) 85–109, doi:10.1146/annurev-anchem-061318-114845.
[45] T. Akyazi, L. Basabe-Desmonts, F. Benito-Lopez, Review on microfluidic paper-based analytical devices towards commercialisation, Anal. Chim. Acta. 1001 (2018) 1–17, doi:10.1016/j.aca.2017.11.010.
[46] S. Nishat, A.T. Jafry, A.W. Martinez, F.R. Awan, Paper-based microfluidics: Simplified fabrication and assay methods, Sensors Actuators, B Chem 336 (2021) 129681, doi:10.1016/j.snb.2021.129681.
[47] M.C. Díaz-Liñán, M.T. García-Valverde, R. Lucena, S. Cárdenas, A.I. López-Lorente, Paper-based sorptive phases for microextraction and sensing, Anal. Methods. 12 (2020) 3074–3091, doi:10.1039/d0ay00702a.
[48] X. Zhu, S. Yuan, Y. Ju, J. Yang, C. Zhao, H. Liu, Water splitting-assisted electrocatalytic oxidation of glucose with a metal-organic framework for wearable nonenzymatic perspiration sensing, Anal. Chem. 91 (2019) 10764–10771, doi:10.1021/acs.analchem.9b02328.
[49] D. Li, X. Cao, Q. Zhang, X. Ren, L. Jiang, D. Li, W. Deng, H. Liu, Facile in situ synthesis of core-shell MOF@Ag electrodes for ultrasensitive SERS detection of polycyclic aromatic hydrocarbons, J. Mater. Chem. A. 7 (2019) 14108–14117, doi:10.1039/c9ta03690c.
[50] Z. Chen, B. Chen, M. He, B. Hu, Magnetic metal-organic framework composites for dual-column solid-phase microextraction combined with ICP-MS for speciation of trace levels of arsenic, Microchim. Acta. 187 (2020) 48, doi:10.1007/s00604-019-4055-8.
[51] N. Alizadeh, A. Salimi, T.K. Sham, CuO/Cu-MOF nanocomposite for highly sensitive detection of nitric oxide released from living cells using an electrochemical microfluidic device, Microchim. Acta. 188 (2021) 1–11, doi:10.1007/s00604-021-04891-1.
[52] R. Guo, L. Xue, G. Cai, W. Qi, Y. Liu, J. Lin, Fe-MIL-88NH2Metal-Organic Framework Nanocubes Decorated with Pt Nanoparticles for the Detection of Salmonella, ACS Appl. Nano Mater. 4 (2021) 5115–5122, doi:10.1021/acsanm.1c00574.
[53] Y.H. Cheng, D. Barpaga, J.A. Soltis, V. Shutthanandan, R. Kargupta, K.S. Han, B.P. McGrail, R.K. Motkuri, S. Basuray, S. Chatterjee, Metal-organic framework-based microfluidic ompedance sensor platform for ultrasensitive detection of perfluorooctanesulfonate, ACS Appl. Mater. Interfaces. 12 (2020) 10503–10514, doi:10.1021/acsami.9b22445.
[54] Y. Zhai, T. Xuan, Y. Wu, X. Guo, Y. Ying, Y. Wen, H. Yang, Metal-organic-frameworks-enforced surface enhanced Raman scattering chip for elevating detection sensitivity of carbendazim in seawater, Sensors Actuators, B Chem 326 (2021) 128852, doi:10.1016/j.snb.2020.128852.
[55] X. Jian, J. Xu, L. Yang, C. Zhao, J. Xu, Z. Gao, Y.Y. Song, Intracellular metal-organic frameworks: Integrating an all-in-one semiconductor electrode chip for therapy, capture, and quantification of circulating tumor cells, Anal. Chem. 92 (2020) 13319–13326, doi:10.1021/acs.analchem.0c02618.
[56] N. Bagheri, H.A.J. Al Lawati, J. Hassanzadeh, Simultaneous determination of total phenolic acids and total flavonoids in tea and honey samples using an integrated lab on a chip device, Food Chem 342 (2021) 128338, doi:10.1016/j.foodchem.2020.128338.
[57] E.E. Ahi, H. Torul, A. Zengin, F. Sucularlı, E. Yıldırım, Y. Selbes, Z. Suludere, U. Tamer, A capillary driven microfluidic chip for SERS based hCG detection, Biosens. Bioelectron. (2022) 195, doi:10.1016/j.bios.2021.113660.
[58] Y. Wang, Z. Mao, Q. Chen, K. Koh, X. Hu, H. Chen, Rapid and sensitive detection of PD-L1 exosomes using Cu-TCPP 2D MOF as a SPR sensitizer, Biosens. Bioelectron. 201 (2022) 113954, doi:10.1016/j.bios.2021.113954.
[59] Q. Wang, Y. Zhao, T. Bu, X. Wang, Z. Xu, H. Zhangsun, L. Wang, Semi-sacrificial template growth-assisted self-supporting MOF chip: A versatile and high-performance SERS sensor for food contaminants monitoring, Sensors Actuators B Chem 352 (2022) 131025, doi:10.1016/j.snb.2021.131025.
[60] Y. Hong, M. Wu, G. Chen, Z. Dai, Y. Zhang, G. Chen, X. Dong, 3D printed micro fluidic device with microporous Mn2O3–modified screen printed electrode for real-time determination of heavy metal ions, ACS Appl. Mater. Interfaces. 8 (2016) 32940–32947, doi:10.1021/acsami.6b10464.
[61] Z. Xu, Z. Liu, M. Xiao, L. Jiang, C. Yi, A smartphone-based quantitative point-of-care testing (POCT) system for simultaneous detection of multiple heavy metal ions, Chem. Eng. J. 394 (2020) 124966, doi:10.1016/j.cej.2020.124966.
[62] O. Halevi, J.M.R. Tan, P.S. Lee, S. Magdassi, Hydrolytically stable MOF in 3D-printed structures, Adv. Sustain. Syst 2 (2018) 1700150, doi:10.1002/adsu.201700150.
[63] R. Li, S. Yuan, W. Zhang, H. Zheng, W. Zhu, B. Li, M. Zhou, A. Wing-Keung Law, K. Zhou, 3D printing of mixed matrix films based on metal-organic frameworks and thermoplastic polyamide 12 by selective laser sintering for water applications, ACS Appl. Mater. Interfaces. 11 (2019) 40564–40574, doi:10.1021/acsami.9b11840.
[64] R. Pei, L. Fan, F. Zhao, J. Xiao, Y. Yang, A. Lai, S.F. Zhou, G. Zhan, 3D-Printed metal-organic frameworks within biocompatible polymers as excellent adsorbents for organic dyes removal, J. Hazard. Mater. 384 (2020) 121418, doi:10.1016/j.jhazmat.2019.121418.
[65] E. Vlachou, A. Margariti, G.S. Papaefstathiou, C. Kokkinos, Voltammetric determination of pb(II) by a Ca-MOF-modified carbon paste electrode integrated in a 3D-printed device, Sensors 20 (2020), doi:10.3390/s20164442.
[66] C. Kokkinos, A. Economou, A. Pournara, M. Manos, I. Spanopoulos, M. Kanatzidis, T. Tziotzi, V. Petkov, A. Margariti, P. Oikonomopoulos, G.S. Papaefstathiou, 3D-printed lab-in-a-syringe voltammetric cell based on a working electrode modified with a highly efficient Ca-MOF sorbent for the determination of Hg(II), Sensors Actuators, B Chem 321 (2020) 128508, doi:10.1016/j.snb.2020.128508.
[67] Z. Liu, X. Xia, W. Li, L. Xiao, X. Sun, F. Luo, Q. Chen, Q. Qian, In situ growth of ca2+-based metal-organic framework on casio3/abs/tpu 3d skeleton for methylene blue removal, Materials (Basel) 13 (2020) 1–14, doi:10.3390/ma13194403.
[68] S. Waheed, M. Rodas, H. Kaur, N.L. Kilah, B. Paull, F. Maya, In-situ growth of metal-organic frameworks in a reactive 3D printable material, Appl. Mater. Today. 22 (2021) 100930, doi:10.1016/j.apmt.2020.100930.
[69] L. Wang, W. Gao, S. Ng, M. Pumera, Chiral Protein-Covalent Organic Framework 3D-Printed Structures as Chiral Biosensors, Anal. Chem. 93 (2021) 5277–5283, doi:10.1021/acs.analchem.1c00322.
[70] N. Bagheri, H.A.J. Al Lawati, N.A. Al Sharji, J. Hassanzadeh, Magnetic zinc based 2D-metal organic framework as an efficient adsorbent for simultaneous determination of fluoroquinolones using 3D printed microchip and liquid chromatography tandem mass spectrometry, Talanta 224 (2021) 121796, doi:10.1016/j.talanta.2020.121796.
[71] Z. Shi, C. Xu, F. Chen, Y. Wang, L. Li, Q. Meng, R. Zhang, Renewable metal-organic-frameworks-coated 3D printing film for removal of malachite green, RSC Adv 7 (2017) 49947–49952, doi:10.1039/c7ra10912a.
[72] W. Liu, O. Erol, D.H. Gracias, 3D Printing of an in situ grown MOF hydrogel with tunable mechanical properties, ACS Appl. Mater. Interfaces. 12 (2020) 33267–33275, doi:10.1021/acsami.0c08880.
[73] M. del Rio, M. Villar, S. Quesada, G. Turnes Palomino, L. Ferrer, C. Palomino Cabello, Silver-functionalized UiO-66 metal-organic framework-coated 3D printed device for the removal of radioactive iodine from wastewaters, Appl. Mater. Today. 24 (2021) 101130, doi:10.1016/j.apmt.2021.101130.
[74] Y. Jiang, P. Ma, H. Piao, Z. Qin, S. Tao, Y. Sun, X. Wang, D. Song, Solid-phase microextraction of triazine herbicides via cellulose paper coated with a metal-organic framework of type MIL-101(Cr), and their quantitation by HPLC-MS, Microchim. Acta. 186 (2019) 742, doi:10.1007/s00604-019-3889-4.

[75] Z. Xia, D. Li, W. Deng, Identification and Detection of Volatile Aldehydes as Lung Cancer Biomarkers by Vapor Generation Combined with Paper-Based Thin-Film Microextraction, Anal. Chem. 93 (2021) 4924–4931, doi:10.1021/acs.analchem.0c05348.
[76] Q. Jiang, Y.J. Chandar, S. Cao, E.D. Kharasch, S. Singamaneni, J.J. Morrissey, Rapid, point-of-Care, paper-based plasmonic biosensor for Zika virus diagnosis, Adv. Biosyst. 1 (2017) 1700096, doi:10.1002/adbi.201700096.
[77] X. Liu, X. Gao, L. Yang, Y. Zhao, F. Li, Metal-Organic Framework-Functionalized Paper-Based Electrochemical Biosensor for Ultrasensitive Exosome Assay, Anal. Chem. 93 (2021) 11792–11799, doi:10.1021/acs.analchem.1c02286.
[78] Y. Hou, C. Lv, W. Liu, Y. Guo, Y. Jin, B. Li, Y. Zhang, Y. Liu, In situ synthesis of copper metal-organic framework on paper-based device for dual-mode detection of volatile sulfur compounds in exhaled breath, Sensors Actuators B Chem 352 (2022) 131008, doi:10.1016/j.snb.2021.131008.
[79] I. Ortiz-Gómez, A. Salinas-Castillo, A.G. García, J.A. Álvarez-Bermejo, I. de Orbe-Payá, A. Rodríguez-Diéguez, L.F. Capitán-Vallvey, Microfluidic paper-based device for colorimetric determination of glucose based on a metal-organic framework acting as peroxidase mimetic, Microchim. Acta. 185 (2018) 47, doi:10.1007/s00604-017-2575-7.
[80] X. Wei, J. Guo, H. Lian, X. Sun, B. Liu, Cobalt metal-organic framework modified carbon cloth/paper hybrid electrochemical button-sensor for nonenzymatic glucose diagnostics, Sensors Actuators B Chem 329 (2021) 129205, doi:10.1016/j.snb.2020.129205.
[81] Z. Li, Y. Xi, A. Zhao, J. Jiang, B. Li, X. Yang, J. He, F. Li, Cobalt-imidazole metal-organic framework loaded with luminol for paper-based chemiluminescence detection of catechol with use of a smartphone, Anal. Bioanal. Chem. 413 (2021) 3541–3550, doi:10.1007/s00216-021-03305-8.
[82] H.A.J. Al Lawati, J. Hassanzadeh, Dual-function 2D cobalt metal-organic framework embedded on paper as a point-of-care diagnostic device: Application for the quantification of glucose, Anal. Chim. Acta. 1139 (2020) 15–26, doi:10.1016/j.aca.2020.09.026.
[83] H. Li, B. Liu, L. Xu, H. Jiao, A hetero-MOF-based bifunctional ratiometric fluorescence sensor for pH and water detection, Dalt. Trans. (2020), doi:10.1039/d0dt03626a.
[84] X.-B. Chen, C.-X. Qi, Y.-B. Xu, H. Li, L. Xu, B. Liu, A quantitative ratiometric fluorescent Hddb-based MOF sensor and its on-site detection of the anthrax biomarker 2,6-dipicolinic acid, J. Mater. Chem. C. (2020), doi:10.1039/d0tc04001k.
[85] X. Yue, Y. Li, S. Xu, J. Li, M. Li, L. Jiang, M. Jie, Y. Bai, A portable smartphone-assisted ratiometric fluorescence sensor for intelligent and visual detection of malachite green, Food Chem 371 (2022) 131164, doi:10.1016/j.foodchem.2021.131164.
[86] Q. Lu, T. Su, Z. Shang, D. Jin, Y. Shu, Q. Xu, X. Hu, Flexible paper-based Ni-MOF composite/AuNPs/CNTs film electrode for HIV DNA detection, Biosens. Bioelectron. 184 (2021) 113229, doi:10.1016/j.bios.2021.113229.
[87] Y. Yang, W. Liu, J. Cao, Y. Wu, On-site, rapid and visual determination of Hg2+ and Cu2+ in red wine by ratiometric fluorescence sensor of metal-organic frameworks and CdTe QDs, Food Chem 328 (2020) 127119, doi:10.1016/j.foodchem.2020.127119.
[88] L. Yu, C. He, Q. Zheng, L. Feng, L. Xiong, Y. Xiao, Dual Eu-MOFs based logic device and ratiometric fluorescence paper microchip for visual H2O2 assay, J. Mater. Chem. C. 8 (2020) 3562–3570, doi:10.1039/c9tc06915a.
[89] S. Nandi, M. SK, S. Biswas, Rapid switch-on fluorescent detection of nanomolar-level hydrazine in water by a diacetoxy-functionalized MOF: application in paper strips and environmental samples, Dalt. Trans. 49 (2020) 12565–12573, doi:10.1039/d0dt02491k.
[90] R. Cui, Y. Wan, G. Ji, Z. Liu, A highly selective and sensitive fluorescent sensor based on Tb3+ functionalized MOFs to determine arginine in urine: A potential application for the diagnosis of cystinuria, Analyst 144 (2019) 5875–5881, doi:10.1039/c9an01204d.
[91] H. Che, Y. Li, S. Zhang, W. Chen, X. Tian, C. Yang, L. Lu, Z. Zhou, Y. Nie, A portable logic detector based on Eu-MOF for multi-target, on-site, visual detection of Eu3+ and fluoride in groundwater, Sensors Actuators, B Chem 324 (2020) 128641, doi:10.1016/j.snb.2020.128641.
[92] C. Zhou, K. Cui, Y. Liu, S. Hao, L. Zhang, S. Ge, J. Yu, Ultrasensitive Microfluidic Paper-Based Electrochemical/Visual Analytical Device via Signal Amplification of Pd@Hollow Zn/Co Core-Shell ZIF67/ZIF8 Nanoparticles for Prostate-Specific Antigen Detection, Anal. Chem. 93 (2021) 5459–5467, doi:10.1021/acs.analchem.0c05134.
[93] S. Li, C. Pang, X. Ma, Y. Zhang, Z. Xu, J. Li, M. Zhang, M. Wang, Microfluidic paper-based chip for parathion-methyl detection based on a double catalytic amplification strategy, Microchim. Acta. 188 (2021) 1–8, doi:10.1007/s00604-021-05084-6.
[94] G.C. Ilacas, A. Basa, K.J. Nelms, J.D. Sosa, Y. Liu, F.A. Gomez, Paper-based microfluidic devices for glucose assays employing a metal-organic framework (MOF), Anal. Chim. Acta. 1055 (2019) 74–80, doi:10.1016/j.aca.2019.01.009.
[95] H. Wang, Y. Jian, Q. Kong, H. Liu, F. Lan, L. Liang, S. Ge, J. Yu, Ultrasensitive electrochemical paper-based biosensor for microRNA via strand displacement reaction and metal-organic frameworks, Sensors Actuators, B Chem 257 (2018) 561–569, doi:10.1016/j.snb.2017.10.188.
[96] K. Vaid, J. Dhiman, S. Kumar, K.H. Kim, V. Kumar, Mixed metal (cobalt/molybdenum) based metal-organic frameworks for highly sensitive and specific sensing of arsenic (V): Spectroscopic versus paper-based approaches, Chem. Eng. J. 426 (2021) 131243, doi:10.1016/j.cej.2021.131243.
[97] G. Zhang, T. Ding, Q. Shi, Z. Jiang, Y. Niu, M. Zhang, L. Tong, Z. Chen, B. Tang, Covalent organic frameworks-based paper solid phase microextraction combined with paper spray mass spectrometry for highly enhanced analysis of tetrabromobisphenol A, Analyst 145 (2020) 6357–6362, doi:10.1039/d0an00759e.
[98] T. Leelasree, V. Selamneni, T. Akshaya, P. Sahatiya, H. Aggarwal, MOF based flexible, low-cost chemiresistive device as a respiration sensor for sleep apnea diagnosis, J. Mater. Chem. B. 8 (2020) 10182–10189, doi:10.1039/d0tb01748e.
[99] Z. Huang, Q. Xu, X. Hu, Covalent organic frameworks functionalized carbon fiber paper for the capture and detection of hydroxyl radical in the atmosphere, Chinese Chem. Lett. 31 (2020) 2495–2498, doi:10.1016/j.cclet.2020.06.017.
[100] R. Tian, Y. Li, J. Bai, Hierarchical assembled nanomaterial paper based analytical devices for simultaneously electrochemical detection of microRNAs, Anal. Chim. Acta. 1058 (2019) 89–96, doi:10.1016/j.aca.2019.01.036.
[101] L. Yu, Q. Zheng, D. Wu, Y. Xiao, Bimetal-organic framework nanocomposite based point-of-care visual ratiometric fluorescence pH microsensor for strong acidity, Sensors Actuators, B Chem 294 (2019) 199–205, doi:10.1016/j.snb.2019.05.037.
[102] S.J. Qin, B. Yan, The point-of-care colorimetric detection of the biomarker of phenylamine in the human urine based on Tb3+ functionalized metal-organic framework, Anal. Chim. Acta. 1012 (2018) 82–89, doi:10.1016/j.aca.2018.01.041.
[103] J. Yan, J. Zhang, M. Zhang, G. Shi, Lanthanide metal-organic framework as a paper strip sensor for visual detection of sulfonamide with smartphone-based point-of-care platform, Talanta 237 (2022) 122920, doi:10.1016/j.talanta.2021.122920.
[104] L. Song, M. Liu, F. Tian, Z. Liu, A Novel Luminescent Metal-Organic Framework as a Remarkable Sensor for Detecting Aristolochic Acids in Biological Fluids, Eur. J. Inorg. Chem. (2021) 1695–1700, doi:10.1002/ejic.202100119.
[105] D.M. Li, S.Y. Zhang, J.Y. Wan, W.Q. Zhang, Y.L. Yan, X.H. Tang, S.R. Zheng, S.L. Cai, W.G. Zhang, A new hydrazone-linked covalent organic framework for Fe(III) detection by fluorescence and QCM technologies, CrystEngComm 23 (2021) 3594–3601, doi:10.1039/d1ce00212k.
[106] D.M. Li, S.Q. Li, J.Y. Huang, Y.L. Yan, S.Y. Zhang, X.H. Tang, J. Fan, S.R. Zheng, W.G. Zhang, S.L. Cai, A recyclable bipyridine-containing covalent organic framework-based QCM sensor for detection of Hg(II) ion in aqueous solution, J. Solid State Chem. 302 (2021) 122421, doi:10.1016/j.jssc.2021.122421.
[107] C. Zhu, D. Liu, Z. Chen, L. Li, T. You, An ultra-sensitive aptasensor based on carbon nanohorns/gold nanoparticles composites for impedimetric detection of carbendazim at picogram levels, J. Colloid Interface Sci. 546 (2019) 92–100, doi:10.1016/j.jcis.2019.03.035.
[108] A.K. Mohammed, S. Usgaonkar, F. Kanheerampockil, S. Karak, A. Halder, M. Tharkar, M. Addicoat, T.G. Ajithkumar, R. Banerjee, Connecting Microscopic Structures, Mesoscale Assemblies, and Macroscopic Architectures in 3D-Printed Hierarchical Porous Covalent Organic Framework Foams, J. Am. Chem. Soc. 142 (2020) 8252–8261, doi:10.1021/jacs.0c00555.
[109] N. Wongkaew, M. Simsek, C. Griesche, A.J. Baeumner, Functional nanomaterials and nanostructures enhancing electrochemical biosensors and lab-on-a-chip performances: recent progress, applications, and future perspective, Chem. Rev. 119 (2019) 120–194, doi:10.1021/acs.chemrev.8b00172.
[110] L.D. Chen, C.Z. Lai, L.P. Granda, M.A. Fierke, D. Mandal, A. Stein, J.A. Gladysz, P. Bühlmann, Fluorous membrane ion-selective electrodes for perfluorinated surfactants: Trace-level detection and in situ monitoring of adsorption, Anal. Chem. 85 (2013) 7471–7477, doi:10.1021/ac401424j.
[111] Y. Zhao, H. Ouyang, S. Feng, Y. Luo, Q. Shi, C. Zhu, Y.C. Chang, L. Li, D. Du, H. Yang, Rapid and selective detection of Fe(III) by using a smartphone-based device as a portable detector and hydroxyl functionalized metal-organic frameworks as the fluorescence probe, Anal. Chim. Acta. 1077 (2019) 160–166, doi:10.1016/j.aca.2019.05.062.
[112] J. Zhang, L. Zhou, Z. Jia, X. Li, Y. Qi, C. Yang, X. Guo, S. Chen, H. Long, L. Ma, Construction of covalent organic framework with unique double-ring pore for size-matching adsorption of uranium, Nanoscale 12 (2020) 24044–24053, doi:10.1039/d0nr06854c.